Heterogeneous investment horizons and realized jump risk in financial markets

Deniz Erdemlioglu[a,*], Nikola Gradojevic[a,b]

[a] *IÉSEG School of Management (LEM-CNRS), France.*
[b] *The Rimini Centre for Economic Analysis, Italy.*

This Version: January 8, 2014

Abstract

We study the transmission of jump-type tail risk across trading horizons. We propose an estimation procedure to identify the regimes of jump risk simultaneously over multiple time scales. Applying our method to data on bonds, stocks and currencies, we find evidence of *regime-shifts* and *horizon-dependence* in jump risk. We show that while the duration of high risk episodes is rather short at intra-day time intervals, risk regimes are persistent at long investment horizons. When sudden shocks occur, the realized risk associated with low frequencies is swiftly absorbed by the traders at high frequencies. This evidence holds for both tail types (right-left) and all markets, although the results indicate that the European bond market is more sensitive to negative (left-tail) jump risk, relative to the US bond market. Finally, by extracting the jump component of the VIX index, we characterize the *jump fear* as combinations of different investment horizons and *vertical clustering* of risk states. Taken together, our results suggest that the premium—tied to compensation for tail (jump) risks—not only depends on the periods of financial stress, but also on investors' trading frequencies.

Keywords: Jumps, Volatility, High-frequency data, Multiple investment scales, Hidden Markov tree models, Wavelets
EFM: 310, 330, 610

---

1. Introduction

Understanding the dynamics of financial markets is challenging because the "true" data generating process is unknown in practice. This limitation has important implications for asset pricing (Aït-Sahalia and Jacod, 2012; Carr et al., 2002), identifying tail events (Bollerslev and Todorov, 2011a,b), estimating risk aversion (Dieckmann and Gallmeyer, 2005), and for optimal portfolio choice (Aït-Sahalia et al., 2009). Moreover, a financial model capturing low frequency data characteristics may not be compatible with high-frequency dynamics (Aït-Sahalia and Jacod, 2011). The model selection hence depends on time scales or, more precisely, on investment horizons of traders.

*Corresponding author. IÉSEG School of Management (LEM-CNRS), Lille Catholic University, 3, rue de la Digue, 59000 Lille, France. Tel: + 32.81.724889. Fax: + 32.81.724840.

Email addresses: d.erdemlioglu@ieseg.fr (Deniz Erdemlioglu), n.gradojevic@ieseg.fr (Nikola Gradojevic)

To investigate these implications and stylized facts, studies usually take two different approaches. While one strand of literature focuses on exploring how markets process new information (see e.g., Andersen et al., 2007b, 2003; Ederington and Lee, 1995, 1993), more recent works employ non-parametric approaches—such as realized volatility—to measure uncertainty and associated market risk characteristics (see e.g., Aït-Sahalia and Jacod, 2012; Aït-Sahalia et al., 2012).

From a practical point of view, estimating and modeling volatility is important because market participants consider trading strategies' exposure to risk during high volatility regimes. However, the models that solely use volatility as a market's "fear gauge" (such as the VIX index) lack the ability to explain price discontinuities or jumps in the data (Aït-Sahalia and Jacod, 2009; Lahaye et al., 2011 and Lee and Hannig, 2010).[1] Incorporating jumps into asset price models is crucial for at least three reasons. First, as the efficient market hypothesis posits, asset prices should react rapidly to news surprises to prevent risk-adjusted profit opportunities. Second, while diffusion volatility has forecasting power for future volatility, jumps might contain no predictive information about volatility or even distort volatility forecasts (Andersen et al., 2007a; Neely, 1999). Third, time-varying diffusion volatility and jumps imply different modeling and hedging strategies (Bollerslev and Todorov, 2011a). In particular, a semimartingale model—with only continuous volatility component—represents a different source of risk when compared to models with jumps. As Bollerslev and Todorov (2011b) and Drechsler and Yaron (2011) show, price spikes and jump events represent tail risk, which require a risk premium that cannot be explained by continuous volatility movements.[2]

Given the importance of jumps, most recent studies deal with two fundamental issues: (1) identification of jump events to measure jump risk, and (2) determinants of jumps.[3] Among these works, Barndorff-Nielsen and Shephard (2004) propose the first technique to pinpoint jump locations, and document evidence that jumps often correspond to days of macroeconomic news announcements. Andersen et al. (2007b, 2003) support this view and show that information arrival affects jump occurrences in asset prices. While these studies examine the jumps-news relationship at a daily frequency, Lee and Mykland (2008) develop a statistical method that precisely identifies jump times and sizes at intra-day frequencies.[4] This technique allows researchers to track the variation in realized jump risk at every instant, based on a predetermined time scale (e.g., 5-minute or 15-minute data). Following the identification approach of Lee and Mykland (2008), Lahaye et al. (2011) show that announcements also explain the simultaneous (or common) jump arrivals in multiple markets.[5] Along those lines, Fagan et al. (2013) develop non-parametric tests—relying on the wavelet methodology—to identify stock price jumps at ultra high frequencies. Overall, three main conclusions emerge from this literature: (*i*) jumps are present in the data (Aït-Sahalia and Jacod, 2012), (*ii*) jump arrivals are linked to news events together with market illiquidity (Dewachter et al., 2014; Fagan et al., 2013; Lahaye et al., 2011), and (*iii*) realized jump risk propagates across financial markets and geographic regions (Aït-Sahalia et al., 2013).

[1] The VIX Index measures the expected market volatility over the next 30 days, based upon the implied volatility that is observed through the prices of S&P 500 index options.

[2] Along those lines, see e.g., Maheu et al. (2013) who study the role of jumps in estimating equity risk premia.

[3] See Neely (2011) for a review on the link between news announcements and jump dynamics.

[4] As Lee and Mykland (2008) argue, the identification of intra-day jumps depends on the underlying data generating process. Lee and Mykland (2008) assume that the price process is a jump-diffusion, but Lee and Hannig (2010) relax this assumption by developing a test statistic to detect intra-day jumps under a Lévy process. In our paper, we focus on the former technique and use the latter for a robustness check.

[5] To estimate cojumps in a multivariate process, see e.g., Jacod and Todorov (2008).

In this paper, we extend these studies by establishing a direct link between jumps and heterogeneity in investors' trading horizons. More specifically, we first characterize the jump regimes in asset prices, and then examine the transition of those *realized* jump risk episodes across multiple investment frequencies ranging from minutes to months. In essence, our approach is motivated by a large body of work on heterogeneous expectations and agent models, including the studies of Boswijk et al. (2007), De Grauwe and Kaltwasser (2012), Jong et al. (2009) and Hommes (2006, 2011), among others. Consider two types of traders, one trading with a short time horizon, and the other with a long time horizon. Short-term traders—such as day/intra-day traders—carry out trades only during the day but do not carry overnight positions; they constantly watch the market, re-evaluate their positions and execute transactions at a high frequency. On the other hand, long-term traders are "fundamentalist-type" investors: they trade on longer time horizons, look at the price variation only once a day or less frequently. The combination of these activities leads to price discovery process which in turn generates realized returns and realized risk in the marketplace (see e.g., Andersen et al., 2007c; Lee and Hannig, 2010).[6]

In such a heterogeneous market environment—with respect to investment horizons, the reaction of traders to new information could be different. For instance, while low-frequency news shocks (such as macro announcements, central bank interventions or forward guidance events) might penetrate through all layers of the entire market, high-frequency news shocks (e.g., asset-specific idiosyncratic news, market microstructure events) are likely to be short-lived without long term impact (Calvet and Fisher, 2007). This implies that a sudden and large price jump might be a major event (and thus represent "jump risk") for day traders, but it may not affect central bankers and long-term traders who usually face the consequences of price jump risk over long time intervals (see e.g., Aït-Sahalia and Jacod, 2012). In fact, long-term traders judge the tail events and jump risk at a coarse time scale whereas short-term traders watch market movements continuously. The propagation of realized (or actual) jump risk across multiple investment horizons may thus develop a channel of information flow between low-frequency and high-frequency time scales. In this study, we aim at capturing such dynamics.

Our paper makes three main contributions to the literature. First, we propose an estimation procedure to identify the regimes of jumps—and associated market risk—across various investment horizons. Relying on the jump test of Lee and Mykland (2008) and Gençay et al. (2010)'s wavelet-based (hidden) Markov model, the procedure determines the scale transition of market "fear risk" that is purely driven by the realized jumps in asset prices. Using data on stock indices, bond futures and the EUR/USD exchange rate, we empirically show that jump risk in financial markets is not only time-varying (see e.g., Dieckmann and Gallmeyer, 2005; Duan and Yeh, 2010; Zhang et al., 2009), but also scale-dependent with "vertical" regime shifts.

Second, we contribute to the literature of heterogeneous expectations and agents. Our empirical motivation is based on a trading mechanism in which two types of traders exchange financial securities (e.g., Chauveau and Subbotin, 2013): a fundamentalist (with long-term investment horizon), and a day trader (with short-term investment horizon). Both types of investors have exposure to jump risk, but the degree of exposure as well as its transition (from one horizon to another) is unobservable in practice: does the jump risk that fundamentalists face impact the risk associated with high-frequency trading? If so, what direction and magnitude of jump risk matter? To answer these questions, one

[6] In this context, see also Hommes et al. (2005) for a comprehensive discussion on how market equilibrium determines the realized prices in an experimental economy with heterogeneous expectations.

needs to differentiate between high and low risk states, and between upside (i.e., "right-tail") risk and downside (i.e., "left-tail") risk. Does jump risk propagation depend on asset classes? In this paper, we tackle these questions empirically. As is well-documented in the literature, market heterogeneity can be related to agents': (*i*) beliefs (e.g., Boswijk et al., 2007; Brock and Hommes, 1998, 1997; De Grauwe and Kaltwasser, 2012), (*ii*) expectations (e.g., Hommes, 2011), and (*iii*) information sets (e.g., Bacchetta and Wincoop, 2006; Dominguez, 2006). Along those lines, we introduce another dimension of heterogeneity by linking realized jump risk "vertically" to different investment horizons.

Third, by studying jump risk across multiple time scales, we further find evidence of *asymmetric risk transmission*. This (cascade) mechanism functions in a way that a *low* jump risk state at a long time horizon is most likely followed by a *low* jump risk state at shorter time horizons. In contrast, a high jump risk state at long time horizons does not necessarily imply a high jump risk state at higher frequencies. A possible explanation for these findings could be that markets tend to absorb (or hedge) jumps at higher frequencies much quicker than they do at lower frequencies. In fact, these results are even more pronounced when we split the realized jump risk into positive ("right-tail") and negative ("left-tail") jump risk components. Among all asset classes, our empirical analysis further indicates that high-frequency traders in the Euro bond market are more sensitive to low-frequency downside jump risk relative to the high-frequency traders of the U.S. bond futures. Stock market, however, is found more prone to downside jump risk compared to currency and bond markets. An important exception to the above-established stylized facts on jump propagation is revealed for the realized jumps in the VIX index: we document "vertical" jump risk clustering where the transitional probabilities suggest that a low (high) jump risk regime in the VIX at a long time horizon will most likely be followed by a low (high) jump risk regime at a shorter time horizon.

On the methodological side, our testing procedure relies on the likelihood estimation of a risk regime at high-frequencies (e.g., 5-minutes) conditional on low-frequencies (e.g., weekly). Similar settings have been adopted in the literature. For instance, Gençay et al. (2001) show that coarse volatility (that captures the actions of long-term traders) predicts the fine volatility (that captures the actions of short-term traders) better than the other way around. The argument for the direction of causality stems from the conjecture that fine volatility does not affect the trading strategies of long-term traders because they typically trade according to the market "fundamentals". Specifically, short-term traders could have a certain influence on the arrival of long-term traders' orders, but not on their investment decisions. Meanwhile, large orders held over longer periods may generate multiplicative cascades in the shorter periods upon their execution (Mandelbrot, 1974). In other words, financial markets present a "turbulence" of volatilities from low to high frequencies. This phenomenon is explained in Lynch and Zumbach (2003) by documenting that traders working at long (short) term horizons use low (high) frequency data. Hence, traders only interact in time, and when a trader at any time horizon decides to trade, volatility surges at the shortest horizons. More recently, O'Hara (2014) argues that in order to stay in business low-frequency traders ought to behave strategically and outsmart high-frequency traders. We extend these studies and empirically test both directions of dependence. Focusing purely on abnormal shocks hitting the markets, find that the realized jump risk flows from low frequencies to high frequencies, and not vice-versa.

The rest of the paper is organized as follows. Section 2 introduces the statistical estimation procedure to identify the jump propagation across time horizons. Section 3 describes the financial market data and reports our empirical results. In Section 4, we present the robustness checks, modifications and extensions. Section 5 concludes our paper.

2. Methodology

2.1. Setup and assumptions

We start by considering a price process which can be characterized by two uncertainty components. As in Andersen et al. (2007c) and Andersen et al. (2007a), we thus assume that asset prices admit a jump-diffusion process. While the first component of this model represents the *diffusive volatility* associated with the normal variation, the second part of it captures jumps reflecting non-normal price moves and tail events. In this process, the log-price $p(t)$ evolves as follows:

$$dp(t) = \mu(t)dt + \sigma(t)dW(t) + \kappa(t)dq(t), \qquad 0 \leq t \leq T, \tag{1}$$

where $dp(t)$ denotes the logarithmic price increment, $\mu(t)$ is the drift, $W(t)$ denotes a standard Brownian motion, and $q(t)$ is a counting process, possibly a non-homogeneous Poisson process independent of $W(t)$. Note that $\kappa(t)$ $(= p(t) - p(t-))$ represents the jump size.[7] The Brownian motion, $W(t)$, jump sizes, $\kappa(t)$, and the counting process, $q(t)$, are independent of each other. In the absence of jumps, the drift $\mu(t)$ and instantaneous volatility $\sigma(t)$ are such that the underlying DGP is an Itô process with continuous sample paths. The drift and diffusion coefficients may not change dramatically over short periods of time.

Furthermore, we assume that the log-price process $p(t)$ in (1) is observed at the discrete points in time. This implies that the continuously compounded ith intra-day return of a trading day t is given by

$$r_{t,i} \equiv p(t + i\Delta) - p(t + (i-1)\Delta) \tag{2}$$

with $i = 1, ..., M$ and trading days $t = 1, ..., T$. Let $M \equiv \lfloor 1/\Delta \rfloor$ denote the number of intra-day observations over the day. Thus, $\Delta = 1/M$ represents the time between consecutive observations.

2.2. Measuring realized jump risk in price variation

To measure realized (or *ex-post*) jump risk, we use the non-parametric jump detection test proposed by Lee and Mykland (2008). This parsimonious technique allows the identification of jumps at an intra-day level. We further apply the method of Boudt et al. (2011) to account for the intra-day periodicity of volatility. The modified test statistic to detect jumps can be then given by

$$Jump_{t,i} \equiv \frac{\mid r_{t,i} \mid}{\hat{s}_{t,i}\hat{f}_{t,i}}, \tag{3}$$

where $r_{t,i}$ is the ith intra-day return of day t, and $s_{t,i}$ is the stochastic component of intra-day volatility. The estimator for $s_{t,i}$ (i.e., $\hat{s}_{t,i}$) is given by

$$\hat{s}_{t,i} = \sqrt{\frac{1}{M-1} BV_t},$$

[7] $p(t-)$ denotes the left-limit of the price process for all t in $[0,T]$. See e.g., Cont and Tankov (2004) for theoretical properties on such specifications.

where BV_t is the bipower variation proposed by Barndorff-Nielsen and Shephard (2004) as a consistent estimator for integrated volatility (under model (1)). That is,

$$BV_t \equiv \mu_1^{-2} \frac{M}{(M-1)} \sum_{i=2}^{M} |r_{t,i}||r_{t,i-1}| \xrightarrow{\mathbb{P}} \int_{t-1}^{t} \sigma^2(s)ds,$$

where $\mu_1 \equiv \sqrt{2/\pi} \simeq 0.79788$. In Equation (3), $\hat{f}_{t,i}$ is the periodic component of intra-day volatility. We estimate $\hat{f}_{t,i}$ by using the non-parametric estimator of Boudt et al. (2011).[8]

Under the null of no jumps (i.e., when there is no price jump risk), the test statistic $Jump_{t,i}$, (3) follows the same distribution as the absolute value of a standard normal variable. As Lee and Mykland (2008) show, we can then infer jumps from the distribution of the statistic's maximum over the sample size.[9] That is, we reject the null of no realized jump risk (at time t) if

$$Jump_{t,i} > G^{-1}(1-\alpha)S_n + C_n, \tag{4}$$

where $G^{-1}(1-\alpha)$ is the $1-\alpha$ quantile function of the standard Gumbel distribution, $C_n = (2\log n)^{0.5} - \frac{\log(\pi)+\log(\log n)}{2(2\log n)^{0.5}}$ and $S_n = \frac{1}{(2\log n)^{0.5}}$, n being the total number of observations (i.e., $M \times T$).

In the first stage of our analysis, we treat these detected jumps (over a pre-determined frequency) as a measure of realized jump risk in markets.[10] In the second stage (described in the next section), we then use the constructed jumps series to analyze the transition of jumps across different investment horizons. We provide the details of the jump detection procedure in Appendix A.

2.3. Estimating the transition of realized jump risk across horizons

Our primary objective is to determine whether the realized jump risk is transmitted from one trading frequency to another. To do so, we first extend the hidden Markov tree (hereafter denoted HMT) model of Gençay et al. (2010) to capture jump dynamics, and second, perform a wavelet decomposition for the constructed realized jumps series. This technique is based on the discrete wavelet transformation (hereafter denoted DWT) which permits the estimation of the underlying joint distribution of the wavelet coefficients.[11] Utilizing the wavelet-HMT model representation, we classify the multi-scale decomposition of the detected realized jumps into a regime of *high* or *low* jump risk.

To proceed, we first define the transition probability of the jump risk across different time scales or horizons.

Definition 1. *The transition probability $p_{s,j}$ is the likelihood of observing a low (high) jump risk state s at time scale j, given that there is a low (high) jump risk state s at time scale j+1 (lower frequency).*

Based on Definition 1, we assume that the transition (probability) matrix of jump risk is scale-dependent

[8]This estimation scheme is robust since it omits returns that might contain jumps to avoid biased estimates of the periodicity. For brevity, we do not present the periodicity estimation procedure yet it is available upon request.

[9]The sample maximum of the absolute value of a standard normal (i.e., $Jump_{t,i}$ in (3)) follows a Gumbel distribution.

[10]See e.g., Lee and Hannig (2010) as another study which identifies the the arrivals of realized jumps that reflect price jump risk.

[11]See Appendix B for the implementation of the procedure and the estimation of wavelet coefficients based on a HMT model.

and it has the following form,

$$A_j = \begin{bmatrix} p_{0,j} & 1-p_{0,j} \\ 1-p_{1,j} & p_{1,j} \end{bmatrix}, \quad \text{for } j = 1, \ldots, J-1.$$

where the *conditional* transition probabilities are given by

$$\left\{ \begin{aligned} p_{0,j} &= P(\text{low jump risk at scale } j \mid \text{low jump risk at scale } j+1) \\ p_{1,j} &= P(\text{high jump risk at scale } j \mid \text{high jump risk at scale } j+1) \\ 1-p_{0,j} &= P(\text{high jump risk at scale } j \mid \text{low jump risk at scale } j+1) \\ 1-p_{1,j} &= P(\text{low jump risk at scale } j \mid \text{high jump risk at scale } j+1) \end{aligned} \right\}. \tag{5}$$

These conditional probabilities reflect the persistence of large and small wavelet coefficients from long time horizons to shorter time horizons, respectively. One parameter of interest is, for instance, $p_{1,j}$.[12] That is, given a high jump risk state at scale $j+1$, how likely is a high jump risk state to persist to scale j? Put differently, if fundamentalist-type investors face severe market uncertainty in the form of jumps, does such a risk trigger turbulence at high-frequency trading horizons?

Given certain properties of the wavelet-HMT (see Appendix B), the full likelihood is given by

$$\begin{aligned} f_{\mathbf{W}}(\mathbf{W}) &= \sum_{\mathbf{S}} \Bigg\{ P(S_{V_J} = s_{V_J}) f_{V_J|S_{V_J}}(v_J)\, P(S_{J,0} = s_{J,0}) f_{W_{J,0}|S_{J,0}}(w_{J,0}) \\ &\quad \times \prod_{j=1}^{J-1} \prod_{n=0}^{N/2^j-1} f_{W_{j,n}|S_{j,n}}(w_{j,n}) P(S_{j,n} = s_{j,n}|S_{j+1,\lfloor n/2 \rfloor}) \Bigg\}, \end{aligned} \tag{6}$$

where $\mathbf{W}$ is the vector of wavelet coefficients $W_{j,n}$, $S_{j,n}$ is the (hidden) random jump state variable with M possible values such that $s \in \{0, 1, \ldots, M-1\}$. Throughout, we further assume that the distribution for $W_{j,n}$ is based on Gaussian probability density functions (PDFs) with mean μ_s and variance σ_s^2. The complete parameter vector for the wavelet-HMT model is then

$$\theta = (p_{0,1}, p_{1,1}, \ldots, p_{0,J}, p_{1,J}, \mu_{0,1}, \sigma_{0,1}^2, \ldots, \mu_{0,J}, \sigma_{0,J}^2 \mu_{1,1}, \sigma_{1,1}^2, \ldots, \mu_{1,J}, \sigma_{1,J}^2), \tag{7}$$

where $p_{i,j} = p_{0,1}, p_{1,1}, \ldots, p_{0,J}, p_{1,J}$ denotes the transition probabilities and (μ, σ^2) are the parameters of the Gaussian mixtures associated with the Gaussian PDFs. We assume that $\mu_{s,j} = 0$ for all s and j.[13]

Given the observed wavelet coefficients $\mathbf{W}$, we use Expected Maximization (EM) algorithm to estimate the parameters θ and distribution of the hidden jump regime states jointly. On the computational side, we follow Crouse et al. (1998) and calculate the log-likelihood of the wavelet HMT (in (6)) by upward-downward algorithm.[14]

[12] We expect the transition probability from low to high jump risk state $(1 - p_{0,j})$ to be quite small, and therefore $p_{0,j} \approx 1$ for most scales.

[13] This is because DWT ensures that the expected value of all wavelet coefficients will be zero when using a wavelet filter of sufficient length.

[14] The upward-downward algorithm is similar to the forward-backward algorithm for hidden Markov chains. See Baum (1972) for detailed discussion on this issue.

3. Empirical analysis

This section describes the data, presents the main hypotheses to be tested, and reports the results of our empirical analysis.

3.1. Data

The financial market data consist of the EUR/USD exchange rate, Dow Jones stock index (DJI), S&P 500 stock index (SPI), 30-year US Treasury bond futures (UST) and 10-year Euro-bond futures (EUB). We obtain the exchange rate data from Olsen & Associates, and Tickdata company provides the trading data on bond futures and Dow Jones index.[15]

For all asset classes, we use 5-minute data over a period from January 1, 2002 to December 31, 2009. As is usual in the literature (see e.g., Dewachter et al., 2014; Lahaye et al., 2011), we omit trading days with too many missing values or low trading activity. Similarly, we deleted week-ends plus certain fixed and irregular holidays, trading days with too many missing values (corresponding to more than one fourth of the data), empty intervals and consecutive prices.[16] We further adjust the financial market data to daylight saving time, considering the time adjustment periods of the US.[17] Appendix C presents the details of the data description and adjustment procedures.

3.2. Testable hypotheses for realized jump risk transition

Section 2 presents the two-step procedure to measure the transition of jump risk between short to long time periods. In the first stage (Section 2.2), we identify the times (and sizes) of realized jumps, and in the second stage (Section 2.3), we estimate a wavelet-HMT model using the detected realized jumps. Empirically, we are now interested in testing for the jump risk transition likelihoods across scales. Let $\mu_{LL}^{(p_{0,j})}$ denote the mean transition probability from *low* jump risk regime (at scale $j+1$) to *low* jump risk stage at scale j (i.e., LL). Further, let $\mu_{LH}^{(1-p_{0,j})}$ denote the mean transition probability again from *low* jump risk regime (at scale $j+1$) but now to *high* jump risk stage at scale j (i.e., LH). Then, we test the following null and alternative hypotheses:

$$H_0^A : \mu_{LL}^{(p_{0,j})} = \mu_{LH}^{(1-p_{0,j})} \qquad vs. \qquad H_1^A : \mu_{LL}^{(p_{0,j})} \neq \mu_{LH}^{(1-p_{0,j})}. \tag{8}$$

Under the H_0^A, low and high jump risk transition probabilities are identical, given the initial jump risk state is *low* (i.e., LL vs. LH). Intuitively, this means that a low jump risk state at a long time horizon (e.g., 1-week) may trigger low *or* high risk with equal chances at short time horizons (e.g., 5-minutes, 10-minutes). We can further consider that the initial jump risk regime is high. In this case, we can thus test whether high jump risk at a long time period is followed by low or high jump risk at a short time period (i.e., HL vs. HH). That is,

$$H_0^B : \mu_{HL}^{(p_{1,j})} = \mu_{HH}^{(1-p_{1,j})} \qquad vs. \qquad H_1^B : \mu_{HL}^{(p_{1,j})} \neq \mu_{HH}^{(1-p_{1,j})}. \tag{9}$$

[15] The raw bond futures and the stock index data sets include all open-close, high-low prices. In our empirical application, we use closing prices.

[16] The holidays include New Year (December 31 - January 2), Martin Luther King Day, Washington's Birthday or Presidents' Day, Good Friday, Easter Monday, Memorial Day, Independence Day, Labor Day, Thanksgiving Day and Christmas (December 24 - 26).

[17] While adjusting the Euro-bond futures data for daylight saving time, we consider the adjustment periods of the Euro area.

Under the H_0^B, low and high jump risk transition probabilities are identical, given the initial jump risk state is *high* (i.e., HL vs. HH). To test H_0^A and H_0^B (Equations (8)−(9)), we use a non-parametric sign test; see e.g., Fatum and Hutchison (2006, 2003); Dewachter et al. (2014). While the hypotheses given in (8)−(9) are based on the equality of mean probability values, we apply the sign test also for the equality of medians. That is, when the initial jump regime is low,

$$H_0^C : \eta_{LL}^{(p_{0,j})} = \eta_{LH}^{(1-p_{0,j})} \quad vs. \quad H_1^C : \eta_{LL}^{(p_{0,j})} \neq \eta_{LH}^{(1-p_{0,j})}, \tag{10}$$

and when the initial jump regime is high,

$$H_0^D : \eta_{HL}^{(p_{1,j})} = \eta_{HH}^{(1-p_{1,j})} \quad vs. \quad H_1^D : \eta_{HL}^{(p_{1,j})} \neq \eta_{HH}^{(1-p_{1,j})}, \tag{11}$$

where η denotes the median values of transition probabilities. Rejections of the null hypotheses H_0^C and H_0^D will indicate the dependence (direction) of realized jump risk across investment horizons.

3.3. Results

3.3.1. Temporal dynamics of realized jumps

We start by analyzing the dynamics of realized jumps in the data. To proceed, we first compute the discretely observed log-return series (Equation (2)) and apply the realized jump test to return series based on the detection rule (Equation (4)). For all asset classes, the sampling rate is 5-minutes—as a base frequency—over a period from January 1, 2002 to December 31, 2009. Table 1 presents the summary statistics on the temporal behavior of the realized jumps in markets.

[Insert Table 1 here]

Panel A of the table indicates that price jumps mostly occur in currencies compared to stock indices and bond futures. Decomposing total jumps into positive and negative jumps, Panel B further shows that the distribution of the jumps is rather symmetric for stock indices and currencies (51%) whereas bond futures exhibit more negative jumps (and thus higher realized *left-tail* risk). In addition to those properties, Table 1 confirms that jumps are rare events (Panel C). That is, the (unconditional) probability of observing an intra-day realized jump ($P(Jumps)(\%)$) is very low, and ranges only between 0.13% and 0.19% across all asset classes. While the jump sizes in the US bond futures are the largest (Panel D), Euro-bond market tends to have relatively small jumps (0.18).

[Insert Figure 1 here]

To visualize the jump characteristics, we plot in Figure 1 the arrival times and sizes of the identified realized jumps. As seen from the figure, the EUR/USD jumps are quite frequent, while the US bond futures and stock indices exhibit relatively large jumps. We identify only a few large jumps in the Euro-bond futures (middle panel). Overall, these statistical properties of realized jumps are consistent with the earlier evidence reported in Lahaye et al. (2011), Lee and Hannig (2010), and Lee and Mykland (2008), among others.

Given the presence of jumps at single time frequency (i.e., 5-minutes), the next step is to calculate the transition probabilities of realized jumps across time horizons. Table 2 presents the wavelet scales ($j = 1, \ldots, 17$) where time horizons span roughly from 10-minutes to more than a year.

[Insert Table 2 here]

As described in Section 2.3, we consider two types of jump risk states: high jump risk state, and low jump risk state. We estimate a (two-state) wavelet-HMT model on a span of $N = 2^j$ dyadic observations. The dyadic-length vector depends on the asset and it is less than or equal to the available total sample size (see Panel A in Table 1). We report and interpret the main findings separately for each asset class.

3.3.2. Jump risk across investment horizons: bond market dynamics

To analyze the transition of jump risk across time scales, we first focus on the bond market and test the hypotheses presented in Equations (8)−(11). For the UST, Table 3 reports the estimated conditional probabilities for the jump risk transition matrix A_j with scales $j = 1, \ldots, 17$.

[Insert Table 3 here]

The table indicates a strong scale dependency in low jump risk states (first column). That is, both mean (0.916) and median (0.948) transitional probabilities for the Low-to-Low (i.e., *LL*) jump regimes are significantly greater than the estimates for the Low-to-High (i.e., *LH*) regimes (0.085 and 0.051 in second column, respectively). We therefore reject the null hypotheses H_0^A and H_0^C for the equality of means and medians, respectively (see Equations (8)−(10)): observing a low jump risk state at horizon j, given that there is a low jump risk state at horizon $j+1$, is—on average—more likely than observing a high jump risk state at horizon j. Nevertheless, when the initial regime is a high jump risk regime, the same transition direction does not hold (third and fourth columns in Table 3). Although High-to-High (i.e., *HH*) probabilities are—on average—slightly greater than the High-to-Low (i.e., *HL*) probabilities, the average difference in magnitude is not statistically significant; both mean and median p-values are larger than 0.05. Intuitively, a high jump risk state at a lower frequency might be followed by *either* a high or a low jump risk state at a higher frequency. We thus cannot reject the null hypotheses H_0^B and H_0^D.

[Insert Figure 2 here]

To illustrate the time evolution of jump risk regimes across scales, we plot in Figure 2 (upper panel) the estimated sequence of UST jump regimes for low jump risk regimes (light rectangles) and high jump risk regimes (dark rectangles). The lower panel of the figure represents the corresponding time series of realized jumps accounting for both positive and negative jumps (in absolute values). Starting from low-frequency (top) time scales, one can observe that high jump risk states gradually become narrower, indicating that their impact on high-frequency time scales is limited. Moreover, while jump risk regimes are more persistent at long investment horizons (see e.g., scales 7-10), the likelihood of regime switching is relatively high at short investment horizons (see e.g., scales 1-5).

The visual inspection also reveals that the duration of jump risk is shorter at high-frequency time intervals than that at low-frequency horizons. Put differently, even though both types of market participants (i.e., *fundamentalists* vs. *noise traders*) face market risk driven by jumps, the effect of risk could be long-lasting for fundamentalists with long investment horizons. This is, however, not the case for intra-day traders: the risk changes between high and low regimes quite frequently (see the upper panel of Figure 2), and it might be thus anticipated (and/or hedged) quickly in practice. The upper panel of the figure further shows that low jump risk states spread across consecutive time scales more consistently compared to high jump risk states.

After examining the total jump risk, we now differentiate between positive (i.e., right-tail) and negative (i.e., left-tail) realized jumps in the UST data. We are interested in analyzing whether or not similar patterns of jump risk propagation between time scales can be discerned for each subsample. Table 4 summarizes the results for both series.

[Insert Table 4 here]

With respect to positive jumps (upper panel), the results accentuate the existence of large transitional probabilities for the Low-to-Low jump states (first column). The mean (0.929) and median (0.981) transitional probabilities for the LL jump regimes are significantly greater than the estimates for the LH regimes (0.07 and 0.018, respectively). Like the estimates for the total jump risk transition, Table 4 indicates that the average transitional probabilities HH and HL are very close to 50%. This reinforces the previous findings related to the uncertainty of propagation of high jump risk states across time scales. That is, the jump risk is mostly transmitted from long investment horizons to short horizons as long as the initial regime is a low risk regime. On the other hand, when the initial regime is a high jump risk regime (third and fourth columns), the realized risk level can be either high or low with equal chances (i.e., 50%). While we reject the null hypotheses H_0^A and H_0^C (with p-values around 0.001), there is no evidence to reject H_0^B and H_0^D (with p-values around 0.993).

The lower panel of Table 4 reports the estimated transition probabilities for the negative realized jumps. The table indicates that the downside jump risk appears to be more dominant in terms of its ability to penetrate short time intervals (i.e., high frequencies). In particular, the average Low-to-Low and High-to-High probabilities for negative jump risk are slightly larger than their counterparts for positive jump risk. Nevertheless, as in the case of total jump risk transition, the only statistically significant mean value is for the Low-to-Low states (i.e., 0.935). Consequently, Panels A−B of Figure 3 resemble Figure 2 and deliver similar messages: jump risk regimes are more persistent at long investment horizons (scales 7-10), and the duration of high jump risk is shorter at high-frequency time intervals (scales 1-5).

[Insert Figure 3 here]

We now turn to examine the scale dependence of jump risk in the Euro-bond futures (EUB). Table 5 displays the estimation results for total jump risk (upper panel) as well as for the positive and negative jump risks, separately (middle and lower panels). As documented for the UST, the transitional risk probabilities for the Low-to-Low jump risk states (i.e., LL) are—on average—significantly greater than those for the Low-to-High jump risk states (i.e., LH). We reject the null hypotheses of no transitional direction H_0^A and H_0^C in (8)−(10). In contrast to the UST, however, the mean probability of changing regimes from high jump risk at time scale j to high jump risk at (shorter) time period $j-1$ is also relatively high and statistically significant at the 10% level (third column in Table 5). The evidence for the median probabilities (0.563) supports these conclusions: we reject the null hypotheses H_0^B and H_0^D (in (9)−(11)) for the Euro-bond futures.

[Insert Table 5 here]

When we split the total realized jumps into two (non-overlapping) positive and negative jump components, the lower panel of Table 5 shows that the *asymmetry* in the High-to-High probabilities stems from negative jumps. That is, while the average transitional probabilities from the High-to-High and High-to-Low states are roughly equal for positive jumps (0.513 and 0.486 respectively), the average transitional probabilities from the High-to-High and High-to-Low states are statistically different at the 10% significance level for negative jumps (0.540 and 0.459 respectively). In particular, the likelihood that a high negative jump risk at a low-frequency will trigger a high negative jump risk at higher frequencies is significantly larger than that for the positive jumps. This finding may thus suggest that the European bond market has been more sensitive to negative (low-frequency) jump risks that had more impact on high-frequency traders over the sample years. In essence, the US bond market is more resilient to high (low-frequency) negative jumps relative to the European bond market.

3.3.3. Jump risk across investment horizons: stock market dynamics

We proceed by analyzing the transition likelihood of stock price jump risk across time horizons. We estimate the wavelet-based Markov model—see (7)—on Dow Jones and S&P 500 index data. Table 6 reports the average conditional probabilities for the scale transition of jump risk embedded in the realized Dow Jones index returns. As previously documented, we construct the realized jump series in prices for $2^{17} = 131,072$ dyadic observations based on 5-minutes sampling frequency.

[Insert Table 6 here]

Similar to the findings for the US Treasury and Euro bond markets, we identify a strong multi-scale dependency in low jump risk states. In particular, the median Low-to-Low probability value—when we use all realized jumps—is 0.967 (first column), which is higher than that for the bond markets. In addition, the median transitional probabilities for both positive (0.979) and negative (0.991) jumps are larger relative to the corresponding bond market probabilities. This result also implies that the Low-to-High probabilities (i.e., LH) are the smallest, that is, technically speaking, given a wavelet coefficient associated with low jump risk, it is very unlikely that the model will produce a wavelet coefficient associated with high jump risk at the lower scale.

Another interesting finding is that the average High-to-Low probabilities (i.e., HL) appear to be larger than the average High-to-High probabilities, which especially true for negative jumps (lower panel). Even though the difference is statistically insignificant, the evidence suggests relative resiliency of the equity market to the negative (left-tail) jump risk. Put differently, high jump risks in the Dow Jones index that originate at lower frequencies do not affect high-frequency traders as much as they do in the bond market.

[Insert Table 7 here]

Table 7 displays the results for the S&P 500 stock market index returns. The estimates of transition likelihood are in line with the findings for all the other prices. The stylized fact about the most likely transition from the Low-to-Low relative to the Low-to-High jump risk states is confirmed. When positive and negative jumps are considered separately, the average Low-to-Low transitional probabilities are even larger, based on both median and mean measures. Although the differences are not statistically significant at the 5% significance level, the results reveal that a high jump risk regime at a given time scale is most probably followed by a high jump risk at the lower time scale. This evidence is weak, however, when we control for the jump direction: the mean and median values in the right half of Table 7 are roughly 0.5 for the negative and positive jumps.

3.3.4. Jump risk across investment horizons: FX market dynamics

The results for the foreign exchange market (Table 8) are comparable to the ones for the bond markets, but not as pronounced. From the first column of Table 8, we conclude that the average conditional probabilities for the Low-to-Low risk states are still relatively high. We reject the null hypotheses H_0^A and H_0^C (in (8)−(10)).

[Insert Table 8 here]

These findings are in line with those previously discussed for the bond and equity markets. The multi-scale dependency among high jump risk states is not as strong as it is in low jump risk states: a high jump risk regime at a given time scale does not guarantee that wavelet coefficients at the lower time scale will be associated with high jump risk. Nevertheless, the conditional probabilities for the negative realized jumps indicate that high downside (or left-tail) jump risk stability is weaker than in the stock market. The median High-to-High negative jump probability (0.506) is statistically greater than the median High-to-Low probability (0.494) at the 10% significance level.

We can conclude that the results for the Low-to-Low risk states are uniform across the asset classes, but that some markets are more sensitive to negative (left-tail) jump risks that penetrate lower time scales. The most sensitive market is the Euro-bond market, followed by the FX market, and the US bond market. Relying on the results for the Dow Jones and S&P 500 index, stock market appears to be the most immune to negative jump risk across all time scales.

3.4. The VIX, fear of jumps and heterogeneity in trading horizons

In the previous sections, we established an empirical link between asset price jumps and heterogeneity in investment horizons. Our objective is now to characterize the jump risk embedded in volatility, and investigate whether or not market fear is related to trading frequencies. This analysis leads to one important implication: if market fear of jump events is associated with different investment horizons, then the compensation for such jump-type tail risks might depend on investors' trading frequencies. This in turn highlights the importance of heterogeneous horizons to understand jump risk premium dynamics.

Before proceeding, it is worth noting that fear is *unobserved* and driven by future expectations of market participants. To tackle this issue methodologically, we use the VIX index—as a proxy—which is observed and forward-looking.[18] Our empirical strategy remains same. We first identify the location and sizes of realized jumps in the VIX index data. We then use the realized jump series to estimate the transition likelihood of jumps across multiple time scales.

3.4.1. Realized jump risk in the VIX

We start by examining the time series properties of realized (intra-day) VIX jumps. How does the jump fear look like? To illustrate the market fear in the form of jumps, Figure 4 plots a detected realized jump in the S&P 500 and VIX index occurred around 17:40 GMT on September 28, 2008.

[18] See e.g., Bollerslev and Todorov (2011b).

This particular date corresponds to the day when House voted against Lehman Brothers bailout. At 17:40 GMT, the S&P 500 index plunges sharply from the level 1165 to 1140 within minutes (upper left panel). Such a negative price drop is further reflected as a large negative return (jump) that tends to trigger consecutive jumps (upper right panel). Visually, we thus observe the patterns of *low* and *high* jump risk regimes surrounding this bad news hitting financial markets.

[Insert Figures 4 and 5 here]

How do market participants react to *jump-creating* negative shocks? As the lower panels of Figure 4 display, market reaction seems to be rather quick: at 17:40 GMT, the VIX jumps significantly and traders' fear intensifies due to bailout announcement. Negative jump in the S&P 500 coincides with a positive jump in the VIX index, confirming the view of Bollerslev and Todorov (2011b) on volatility jump dynamics. On Figure 5, we plot another realized jump in the S&P 500 and VIX, occurred around 19:45 GMT on May 6, 2010; the day of flash crash. The right panels of the figure present a noticeable feature: while price increments appear to be rather small before the crash (i.e., *low risk regime*), prices and volatility exhibit sudden changes following the flash crash, indicating a *high risk regime* driven purely by realized jumps.

[Insert Table 9 here]

Finally, Table 9 reports the descriptive statistics on the jump components of the S&P 500 and VIX index. From the table, following jump characteristics emerge. First, volatility jumps more often than does price (Panel A). While we identify 107 realized jumps in the S&P 500, there are 340 jumps occurred in the VIX index during this period (Panel B). Second, distributions of jumps appear to be symmetric: negative and positive jump likelihoods are close to each other for both series (Panel C). Third, as Panel D indicates, the sizes of the VIX jumps are larger than that of S&P 500 jumps. Overall, these statistical properties of volatility and price jumps are in line with the results reported in other studies.[19]

3.4.2. Does jump fear depend on investment horizons?

Having studied the temporal dynamics of S&P 500 and VIX jumps, we now examine the propagation of *volatility* jump risk across different investment horizons. Table 10 presents the results for the VIX.

[Insert Table 10 here]

In general, the finding about the high and statistically significant average transition probability from the Low-to-Low jump risk states relative to the Low-to-High jump risk states holds. It is worthwhile to note that the average probabilities in the first column are slightly lower than those for all asset classes. Further, the average transition probabilities from the High-to-High jump risk states are statistically significantly greater than the average transition probabilities from the High-to-Low jump risk states at the 10% significance level. This feature is unique to the VIX and is not observed for any other time series. A more careful investigation reveals that such findings originate from the positive jumps and are not the characteristic of negative jumps. Indeed, the bottom panel of Table 10 shows the average High-to-High and High-to-Low transition probabilities that are not statistically different from each other (0.533 and 0.466; 0.556 and 0.443). Meanwhile, the corresponding probabilities in the middle panel of Table 10 are statistically different at the 10% significance level (0.591 and 0.408; 0.578 and 0.421).

[19]See e.g., Duan and Yeh (2010); Todorov and Tauchen (2011).

[Insert Figure 6 here]

To examine the VIX jump propagation visually, we plot the sequences of jump states in Figure 6. First, one can notice that jumps in the VIX are very frequent, which is not the case with other time series of jumps. Another unique characteristic of the VIX is that black (i.e., high jump risk) regions occupy relatively large areas and vertically penetrate all time scales. More specifically, black (white) rectangles are more likely to be followed by black (white) rectangles across time scales than by white (black) rectangles. This implies that a low (high) jump risk regime in the VIX at a long time horizon will most likely be followed by a low (high) jump risk regime at a shorter time horizon. Thus, our analysis highlights the novel property of the time series of jumps in the VIX, namely its symmetric *vertical dependence*. The VIX data reveal that vertical jump (fear) clustering occurs for both high and low jump risk regimes.

4. Robustness checks and extensions

To examine the robustness of our results, we consider several modifications and extensions. First, relying on the spectrum analysis of Aït-Sahalia et al. (2012), we check whether or not the data generating process (in Equation (1)) is realistic. Second, we identify the arrival times of realized jumps by using two alternative approaches: (i) Bollerslev et al. (2013) threshold approach, and (ii) Lee and Hannig (2010) Lévy jump test. Third, we assess the impact of sample size variation on the estimations. We consider two sub-samples (e.g., normal period vs. crisis) and further extend the sample length. Finally, we modify the setup—in (5)—and estimate the risk transition from high- to low-frequencies.

4.1. Model selection using spectrum analysis

In Section 2, we identified the arrival times and sizes of realized jumps assuming that prices follow a jump-diffusion process (Equation (1)). To check the validity of this assumption, we use the model selection (spectrum) tests of Aït-Sahalia et al. (2012) and examine which components are present in the real data. For each asset class, we consider four model selection tests: (a) testing for the Brownian (continuous) component, (b) testing for the jump (discontinuous) component, (c) testing for the jump activity, (d) testing for the jump frequency. Table 11 reports the results of these tests.

[Insert Table 11 here]

The main message of table is that both Brownian and jump risk components are present in the data, presenting evidence in favor of a jump-diffusion process (second and third columns). For all asset classes, jump activity appears to be finite and the frequency of jumps is rather low, ranging from 0.20 to 0.90 (fifth column). This implies that a compound Poisson process—as we adopt in Section 2—seems to be consistent with the data. Finally, as the last column of the table indicates, jumps represent a significant proportion of the total price variation (25-30%), and volatility jumps more frequently than do prices (41%).

4.2. Alternative tests for identifying realized jumps

We now assess whether our results depend on the jump identification method. For that purpose, we employ the threshold method of Bollerslev et al. (2013) **BTL**) and also the Lévy jump test proposed by Lee and Hannig (2010) (**LH**). While the **BTL** method allows us to account for the impact of small jumps, the **LH** identifies big jumps. Implementing those techniques to our data, we can thus have a global view about whether the base results are immune to relatively large/small jumps in the data.

[Insert Table 12 here]

For both jump detection methods, Table 12 provides key statistics for the S&P 500 index that are compared to the results from Table 7. As before, the S&P 500 index returns are sampled at the 5-min frequency over the entire sample period. The table indicates that the transitional probabilities remarkably resemble those from Table 7 regardless of the jump detection approach. The average Low-to-Low probabilities remain high (above 90%) and are statistically different from the average Low-to-High probabilities that are always below 10%. As in Table 7, when positive and negative jumps are bulked together, there exists a mild, statistically insignificant tendency for the average High-to-High probabilities to appear larger than the average High-to-Low probabilities. When positive and negative jumps are separated, this characteristic disappears.[20] We conclude that our main findings do not depend on the selection of jump estimation methodology.

4.3. Varying sample size and sample period

To investigate the robustness of our results to the sample size and period, we consider the following time periods: extended sample (2002−2013), sub-sample 1 (2002−2006) and sub-sample 2 (2006−2009). Consistent with the previous sub-section, we estimate the time series of jumps for the 5-min S&P 500 index returns independently for each time period. The focus is on all jumps (positive and negative combined) and only negative jumps. Table 13 reports the results in six panels. The top two panels represent the extended sample, the middle is dedicated to the first sub-sample, and the bottom two panels are for the second sub-sample.

[Insert Table 13 here]

We find that the previously established stylized facts for the S&P 500 index are immune to both the extended sample selection and the choice of sub-periods. Although we expected some unique characteristics of the jump propagation during the 2006−2009 period, there are no statistically significant differences compared to the evidence in Table 7. The average transitional probabilities of the Low-to-Low jump risk regime remain statistically greater than the average probabilities of the Low-to-High jump risk regime across all samples.

In terms of negative jumps over the sub-samples, the evidence points to a noticeable opposite behavior of the average probabilities for the High-to-High and High-to-Low jump risk regimes. Specifically, the 2002−2006 period is marked by an increased average transitional probability for the High-to-High negative jump risk regimes, whereas an increased average transitional probability for the High-to-Low negative jump risk regime is pronounced over the 2006−2009 period. This suggests that the market was more sensitive to negative jumps in the 2002−2006 period relative to the 2006−2009 period. Put differently, despite the sub-prime crisis, the market in 2006−2009 stabilized at higher frequencies earlier

[20]For brevity reasons, we do not display the results for positive jumps, but they also exhibit robustness across the jump detection methods.

than it did at lower frequencies. This may be due to possible informational advantages of high-frequency trading concerning the crisis of 2008.[21]

4.4. Characterizing the information flow: risk propagation from low- to high-frequencies

Recall that our base estimation technique relies on a transition likelihood from long to short investment horizons (see (5) in Section 2.3). We now relax this assumption and consider a reverse transition setup such that realized jump risk at high-frequencies may impact low-frequency trading. For consistency with the previous results, we utilize the realized jumps for the 5-min S&P 500 index returns over the 2002−2009 period. We perform this exercise is to verify that the jump risk generated by short-term traders has a limited influence on the long-term traders.[22]

[Insert Table 14 here]

Table 14 shows that for both high and low jump risk states at higher frequencies most likely penetrate lower frequencies as low jump risk states. In particular, the average probabilities for the Low-to-Low and High-to-Low jump risk regimes are dominant and statistically greater than the average probabilities for the Low-to-High and High-to-High jump risk regimes, respectively. Alternatively stated, jump risk originating from higher frequencies has a limited impact on lower frequencies where it quickly becomes absorbed into a low risk regime. This is an important finding that demonstrates the validity of our assumption about the direction of interaction between traders at different investment horizons in terms of the jump risk propagation. Table 14 shows that the average probabilities for the Low-to-Low and High-to-Low jump risk regimes are dominant and statistically greater than the average probabilities for the Low-to-High and High-to-High jump risk regimes, respectively. Alternatively stated, jump risk originating from higher frequencies has a limited impact on lower frequencies where it quickly becomes absorbed into a low risk regime. This result confirms the validity of our likelihood setup—in (5)—for the direction of interaction between traders at different investment horizons in terms of the jump risk propagation.

5. Conclusion

We propose an estimation procedure to identify the propagation of jump risk between short and long investment horizons. The procedure allows us to explicitly test the likelihood of observing a realized jump risk regime at a given time scale conditional on another. We implement this methodology on market data and examine the scale characteristics of jump cascades occurring both in the asset prices and in the VIX volatility index.

Three main results emerge from our empirical analysis. First, we find strong evidence for the “vertical” jump risk propagation across different time horizons. The direction of the transmission mechanism is such that jump risk from longer time horizons (e.g., monthly) influences shorter time horizons (e.g., daily). On the contrary, the activity of high-frequency traders—due the jump risk—has a minor impact on the low-frequency traders. We thus conclude that when sudden shocks arrive, the

[21] These differences in transitional probabilities are, however, statistically insignificant at the 5% significance level.

[22] Technically, we estimate the transition probabilities that the state varable that consists of wavelet coefficients at the lower frequency ($S_{j-1,n}$) is in jump risk state s, given the vector of wavelet coefficients at the higher frequency ($S_{j,n}$) is in jump risk state r ($r, s \in \{High, Low\}$).

trading actions of long term investors amplify the actual risk at the shortest horizons to a greater extent. The evidence for the reverse transmission is, however, rather weak.

Second, the temporal variation in the jump risk exhibits two distinct *jump fear* episodes: high risk versus low risk. While the low jump risk regimes tend to be more persistent at all time horizons, the chance of a regime change from a high jump risk state is rather high at short time horizons. This result thus suggests that even though all investors are exposed to the market jump risk, the impact of risk could be more pronounced for fundamental traders relative to day traders. That is, at high-frequency time scales, the risk changes from high to low states quite frequently, and can be anticipated and hedged quickly in practice. Long-term investors, on the other hand, react to jump-creating news shocks with delays.

Finally, when we decompose the total jump risk into left-tail and right-tail components, the data reveal the fact that European bond market is more prone to downside jump risk relative to the US bond market. Stocks and currencies, however, show strong resiliency to risk stemming purely from negative realized jumps. The propagation of realized jump risk for the VIX index is quite unique in the sense that it exhibits "vertical clustering" where both high and low risk levels at low frequencies are more likely to remain unchanged at higher frequencies.

Several research questions still remain unanswered. For instance, what drives realized risk transition across trading horizons? Is the scale dependence of jump risk associated with macro news (Andersen et al., 2007b, 2003; Lahaye et al., 2011), market microstructure (Fagan et al., 2013), or central banks' forward guidance (Dewachter et al., 2014)? From the standpoint of practitioners, it is also important to understand whether or not the compensation for jump risk (or premium) varies with the investment horizon. Along the lines of Bhamra and Uppal (2014), one could study jump risk (premium) dynamics through a continuous-time general equilibrium model where agents differ with respect to their investment horizons. Lastly, if jump risk insurance depends on the level of risk aversion—as documented by Dieckmann and Gallmeyer (2005), it would be interesting to further explore who is more risk averse towards jump risk: long-term investors or high-frequency traders. We leave these issues for future research.

Acknowledgments

We thank Torben Andersen, Louis Eeckhoudt, Ramo Gençay, John Maheu, Christopher Neely and conference participants at the 8th International Conference on Computational and Financial Econometrics (CFE 2014) for valuable comments and helpful suggestions.

Appendix

A. Realized jumps detection procedure

The intuition behind the jump test proposed simultaneously by Andersen et al. (2007c) and Lee and Mykland (2008) is straightforward: in the absence of jumps, instantaneous returns are increments of the Brownian motion. Standardized returns that are too large to plausibly come from a standard Brownian motion must reflect jumps.[23]

[23] The drift is nearly zero and can be ignored in practice.

More formally, assume we have T days of $\lfloor 1/\Delta \rfloor \equiv M$ equally-spaced intra-day returns and denote the i-th return of day t by $r_{t,i} \equiv p(t+i\Delta) - p(t+(i-1)\Delta)$, where $i = 1, \ldots, M$. Andersen et al. (2007c) and Lee and Mykland (2008) propose the following test statistic for jumps in $r_{t,i}$:

$$J_{t,i} \equiv \frac{\mid r_{t,i} \mid}{\sigma_{t,i}}. \tag{12}$$

In order to implement this test, one must to estimate the unobserved spot volatility $\sigma_{t,i}$ with a robust-to-jumps estimator. Barndorff-Nielsen and Shephard (2004) show that, under weak conditions, realized bipower variation (RBV) converges to integrated volatility under the model described by Equation (1).

$$\operatorname*{plim}_{\Delta \to 0} BV_t(\Delta) = \int_{t-1}^{t} \sigma^2(s)ds, \tag{13}$$

where

$$BV_t(\Delta) \equiv \mu_1^{-2} \frac{M}{(M-1)} \sum_{i=2}^{M} |r_{t,i}||r_{t,i-1}|, \tag{14}$$

with $\mu_1 \equiv \sqrt{2/\pi} \simeq 0.79788$.

Andersen et al. (2007c), Lee and Mykland (2008) propose replacing $\sigma_{t,i}$ in Equation (12) by $\hat{s}_{t,i}$, i.e., the average of the RBV computed over a local window length about 1 day, preceding period t, i.

Estimating volatility using RBV rolling windows inappropriately smooths these periodic patterns, because such an estimator is necessarily slowly time-varying. Boudt et al. (2011) show that such cyclical patterns might induce the $J_{t,i}$ statistic to spuriously detect jumps. To correctly infer jumps, we must estimate and remove this deterministic periodicity with a robust-to-jumps volatility estimator.

Following Boudt et al. (2011), we assume that the instantaneous volatility in Equation (1) is the product of a slowly varying component, $\delta(t)$, and a deterministic circadian component, $f(t)$, i.e.,

$$\sigma(t) = \delta(t)f(t). \tag{15}$$

We assume, without loss of generality, this deterministic variance process integrates to one on a daily basis,

$$\int_{t-1}^{t} f^2(s)ds = 1, \tag{16}$$

and standardize the estimates of volatility periodicity accordingly.

B. The wavelet hidden model and its implementation

The discrete wavelet transformation (DWT) is a subsampling of the wavelet coefficients $w(\lambda, t)$ with only dyadic scales, i.e., λ is of the form 2^{j-1}, $j = 1, 2, 3, \ldots$ and, within a given dyadic scale 2^{j-1}, t's are separated by multiples of 2^j.

Let $\mathbf{x}$ be a dyadic length vector ($N = 2^J$) of observations. The length N vector of discrete wavelet coefficients $\mathbf{w}$ is obtained by

$$\mathbf{w} = \mathcal{W}\mathbf{x},$$

where $\mathcal{W}$ is an $N \times N$ real-valued orthonormal matrix (based on the wavelet type) defining the DWT which satisfies $\mathcal{W}^T\mathcal{W} = I_N$ ($n \times n$ identity matrix).[24] The nth wavelet coefficient w_n is associated with a particular scale and with a particular set of times. The vector of wavelet coefficients may be organized into $J+1$ vectors,

$$\mathbf{w} = [\mathbf{w}_1, \mathbf{w}_2, \ldots, \mathbf{w}_J, \mathbf{v}_J]^T,$$

[24]Since DWT is an orthonormal transform, orthonormality implies that $\mathbf{x} = \mathcal{W}^T\mathbf{w}$ and $||w||^2 = ||x||^2$.

where $\mathbf{w}_j$ is a length $N/2^j$ vector of wavelet coefficients associated with changes on a scale of length $\lambda_j = 2^{j-1}$ and $\mathbf{v}_J$ is a length $N/2^J$ vector of scaling coefficients associated with averages on a scale of length $2^J = 2\lambda_J$.

Using the DWT, we may formulate an additive decomposition of $\mathbf{x}$ by reconstructing the wavelet coefficients at each scale independently. Let $\mathbf{d}_j = \mathcal{W}_j^T \mathbf{w}_j$ define the jth level *wavelet detail* associated with changes in $\mathbf{x}$ at the scale λ_j (for $j = 1, \ldots, J$). The wavelet coefficients $\mathbf{w}_j = \mathcal{W}_j \mathbf{x}$ represent the portion of the wavelet analysis (decomposition) attributable to scale λ_j, while $\mathcal{W}_j^T \mathbf{w}_j$ is the portion of the wavelet synthesis (reconstruction) attributable to scale λ_j. For a length $N = 2^J$ vector of observations, the vector $\mathbf{d}_{J+1}$ is equal to the sample mean of the observations.

A multiresolution analysis (MRA) may now be defined via

$$x_t = \sum_{j=1}^{J+1} \mathbf{d}_{j,t} \quad t = 1, \ldots, N. \tag{17}$$

That is, each observation x_t is a linear combination of wavelet detail coefficients at time t. Let $\mathbf{s}_j = \sum_{k=j+1}^{J+1} \mathbf{d}_k$ define the jth level *wavelet smooth*. Whereas the wavelet detail $\mathbf{d}_j$ is associated with variations at a particular scale, $\mathbf{s}_j$ is a cumulative sum of these variations and will be smoother and smoother as j increases. In fact, $\mathbf{x} - \mathbf{s}_j = \sum_{k=1}^{j} \mathbf{d}_k$ so that only lower-scale details (high-frequency features) from the original series remain. The jth level *wavelet rough* characterizes the remaining lower-scale details through

$$\mathbf{r}_j = \sum_{k=1}^{j} \mathbf{d}_k, \qquad 1 \le j \le J+1.$$

The wavelet rough $\mathbf{r}_j$ is what remains after removing the wavelet smooth from the vector of observations. A vector of observations may thus be decomposed through a wavelet smooth and rough via

$$\mathbf{x} = \mathbf{s}_j + \mathbf{r}_j,$$

for all j.

The terminology "detail" and "smooth" were used by Percival and Walden (2000) to describe additive decompositions from Fourier and wavelet transforms. The goal is to look at data at different resolutions with this representation. The smooth part is coarse: we are looking at local averages, i.e., low-frequency trends and the sample mean. The detail is deviation from the smooth part.

Remark 1. In the context of signal processing applications, Crouse et al. (1998) proposed a variety of hidden Markov models for wavelet decompositions of one- and two-dimensional data sets (time series and images). The assumption of uncorrelated wavelet coefficients was replaced by the possibility of allowing correlation between scales of the DWT or within scales of the DWT. The assumption of Gaussianity was also replaced by specifying a small number of unobserved (hidden) states, and representing the distribution of wavelet coefficients as a mixture of Gaussian distributions conditional on the hidden state variable.

Remark 2. One possible model of dependence between wavelet coefficients is to allow association between scales but not within scales. This so-called wavelet hidden Markov tree (HMT) model takes advantage of the persistence of large or small wavelet coefficients across scales with the state variables are connected vertically between scales. Let $\mathbf{W}$ be a vector of wavelet coefficients from a dyadic length vector of observations $\mathbf{X}$. The first point is that the DWT coefficients may be organized into a binary tree, denoted by

$$\mathcal{T} = \{(j, n) : j = 0, \ldots, J; n = 0, \ldots, 2^j - 1\}.$$

The wavelet coefficient $W_{J,0}$ is the root of the tree with children $W_{J-1,0}$ and $W_{J-1,1}$ (the only two wavelet coefficients at scale λ_{J-1}), $W_{J-1,0}$ has children $W_{J-2,0}$ and $W_{J-2,1}$, and so on. The wavelet HMT model is directional in that information from longer time horizons directly influences shorter time horizons, but not vice-versa.

We impose the following five properties on the structure of our wavelet HMT model (Durand and Gonçalvès, 2001):

1. The wavelet coefficient W is modeled by a mixture distribution with probability density function

$$f_W(w) = \sum_{s=0}^{M-1} f_{W|S}(w \mid S = s) P(S = s), \tag{18}$$

where S is a discrete random variable (the hidden state) with M possible values.
2. Let $\mathbf{S} = (\mathbf{S}_1, \ldots, \mathbf{S}_J, \mathbf{S}_{V_J})^T$ define the state vector associated with the vector of wavelet coefficients $\mathbf{W}$, indexed in the same way. Thus, the state vector may be organized as a binary tree rooted at $S_{J,0}$ and read from right to left. Since we are using two indices, one for the scale and one for the location within scale, the parent of $S_{j,n}$ is given explicitly by $S_{j+1,\lfloor n/2 \rfloor}$ for $j = 2, \ldots, J$.[25] The children of $S_{j,n}$ are given explicitly by $S_{j-1,2n}$ and $S_{j-1,2n+1}$. The root is $S_{J,0}$, the next level down from left to right is $S_{J-1,0}$ and $S_{J-1,1}$; the next level down is $S_{J-2,0}$, $S_{J-2,1}$, $S_{J-2,2}$ and $S_{J-2,3}$; and so on.
3. The state variable $S_{j,n}$ is independent of all other states given its parent and children; i.e.,

$$P(S_{j,n} \mid \{S_{a,b}\}_{a \neq j, b \neq n}) = P(S_{j,n} \mid S_{j+1,\lfloor n/2 \rfloor}, S_{j-1,2n}, S_{j-1,2n+1}).$$

4. The joint probability distribution of the wavelet coefficient vector $\mathbf{W}$ is independent given the state vector $\mathbf{S}$; i.e.,

$$f_{\mathbf{W}|\mathbf{S}}(\mathbf{W}) = \prod_{(j,n) \in \mathcal{T}} f_{W_{j,n}|\mathbf{S}}(w_{j,n}).$$

5. The wavelet coefficient $W_{j,n}$ is independent of all other states given its own state; i.e.,

$$f_{W_{j,n}|\mathbf{S}}(w_{j,n}) = f_{W_{j,n}|S_{j,n}}(w_{j,n}) \quad \text{for all } (j,n) \in \mathcal{T}.$$

The last two properties are known as conditional independence properties.

Remark 3. The wavelet HMT model is such that dependence between wavelet coefficients is allowed only between scales. That is, if one pictures a binary tree associating wavelet coefficients , there are no links between adjacent wavelet coefficients within scales – only between and then only from coarse to fine resolution in time. The intuition behind this dependence structure is that if there exists a large wavelet coefficient at a given time horizon (implying a local oscillation with a large amplitude), then at least one of the wavelet coefficients computed using the same data at a shorter time horizon will also be large. That being said, the transition probabilities and parameters of the corresponding mixture distribution are estimated using all wavelet coefficients across time. In this respect, the model uses all available information for parameter estimation, since all wavelet coefficients are used.

C. Description and adjustment of financial data

The EUR/USD exchange rate data set consists of 5-minute intervals of the close-mid prices, based on a 24-hour trading activity (see e.g., Bollerslev and Domowitz, 1993 for a discussion on the high-frequency intra-day dynamics of the foreign exchange markets). As in Andersen and Bollerslev (1998), each currency trading day t begins at 21:00 GMT of the previous trading day $t-1$, and ends at 21:00 GMT of the trading day t. This implies that each FX trading day in our sample $t = 1, 2, ..., T$ has $N = 288$ five minute intra-day prices.

30-year US T-bond futures and 10-year Euro-bond futures are traded on the Chicago Board of Trade (CBOT) and EUREX, respectively. The original time zone for the US bond futures is based on the Eastern time (EST), and we start sampling from 8:30 EST until 15:00 EST, the last observation of the trading day t. These trading hours leave us $N = 78$ five-minute intervals for the all sample trading

[25] $\lfloor x \rfloor$ refers to the floor function of x which is the greatest integer in x, i.e., the largest integer less than or equal to x.

days of 30-year US T-bond futures. For the 10-year Euro-bond futures, the raw data time zone is Europe-Berlin time. The trading hours of the EUREX bond futures contracts span the hours 8:30 CET - 17:30 CET, implying that each trading day $t = 1, 2, ..., T$ consists of $N = 108$ five-minute intervals (CET = GMT + 1 hour).

To be consistent with the currency and the FX news data sets, we convert the original time zones (i.e., EST for the US Bond futures and CET time for the Euro-bond futures contracts) to the Greenwich time (GMT), and take into account the day sessions as well as the trading at both pit and electronic platforms. Overnight sessions are excluded and automatic rolling method is applied to the both 30-year US T-bond and 10-year Euro-bond futures contracts. This method automatically determines the best times to roll of a continuous-time futures price series. The method first computes the daily volume of the both current-month and next-month contracts. Next, the current month contracts are rolled to the next-month contracts, when the volume of the new contracts exceeds the the volume of the current ones. For the both types of assets, we select the contracts as front futures contracts. Those contracts are the contracts that are closest to maturity. The use of the front contracts allows us to process all nearest contracts into a single continuous contract. The raw futures data is obtained as tick data. We create a database for 5-minute intervals by converting tick-by-tick data into intra-day 5-minute frequencies.

The Dow Jones index is a cash level index. We consider the business hours (i.e., the day session) as its period of trading activity, and hence start sampling from 9:30 EST until the market closes at 16:00 EST of the trading day t. This corresponds to $N = 78$ 5-minute intervals, as in the 30-year T-bond futures data. We convert the original time zone of the Dow Jones index to GMT time in order to be consistent with the other financial asset data sets.

References

Aït-Sahalia, Y., Cacho-Diaz, J., Hurd, T.R., 2009. Portfolio choices with jumps: A closed-form solution. Annals of Applied Probability 19, 556–584.

Aït-Sahalia, Y., Cacho-Diaz, J., Laeven, R., 2013. Modeling financial contagion using mutually exciting jump processes. Princeton University, Working Paper.

Aït-Sahalia, Y., Jacod, J., 2009. Testing for jumps in a discretely observed process. Annals of Statistics 37, 184–222.

Aït-Sahalia, Y., Jacod, J., 2011. Testing whether jumps have finite or infinite activity. Annals of Statistics 39, 1689–1719.

Aït-Sahalia, Y., Jacod, J., 2012. Analyzing the spectrum of asset returns: Jump and volatility components in high frequency data. Journal of Economic Literature 50, 1007–1050.

Aït-Sahalia, Y., Jacod, J., Li, J., 2012. Testing for jumps in noisy high frequency data. Journal of Econometrics 168, 202–222.

Andersen, T.G., Bollerslev, T., 1998. DM-Dollar volatility: Intraday activity patterns, macroeconomic announcements and longer run dependencies. Journal of Finance 53, 219–265.

Andersen, T.G., Bollerslev, T., Diebold, F.X., 2007a. Roughing it up: Including jump components in the measurement, modelling and forecasting of return volatility. The Review of Economics and Statistics 89, 701–720.

Andersen, T.G., Bollerslev, T., Diebold, F.X., Vega, C., 2003. Micro effects of macro announcements: Real-time price discovery in foreign exchange. American Economic Review 93, 38–62.

Andersen, T.G., Bollerslev, T., Diebold, F.X., Vega, C., 2007b. Real-time price discovery in stock, bond and foreign exchange markets. Journal of International Economics 73, 251–277.

Andersen, T.G., Bollerslev, T., Dobrev, D., 2007c. No-arbitrage semi-martingale restrictions for continuous-time volatility models subject to leverage effects, jumps and i.i.d. noise: Theory and testable distributional implications. Journal of Econometrics 138, 125–180.

Bacchetta, P., Wincoop, E.V., 2006. Can information heterogeneity explain the exchange rate determination puzzle? American Economic Review 96, 552–576.

Barndorff-Nielsen, O.E., Shephard, N., 2004. Power and bipower variation with stochastic volatility and jumps (with discussion). Journal of Financial Econometrics 2, 1–37.

Baum, L., 1972. An inequality and associated maximization technique in statistical estimation of probabilistic functions of Markov processes. Inequalities 3, 1–8.

Bhamra, H., Uppal, R., 2014. Asset prices with heterogeneity in preferences and beliefs. Review of Financial Studies 27, 519–580.

Bollerslev, T., Domowitz, I., 1993. Trading patterns and prices in the interbank foreign exchange market. Journal of Finance 48, 1421–1443.

Bollerslev, T., Todorov, V., 2011a. Estimation of jump tails. Econometrica 79, 1727–1783.

Bollerslev, T., Todorov, V., 2011b. Tails, fears and risk premia. Journal of Finance 66, 2165–2211.

Bollerslev, T., Todorov, V., Li, S.Z., 2013. Jump tails, extreme dependencies and the distribution of stock returns. Journal of Econometrics 172, 307–324.

Boswijk, H.P., Hommes, C.H., Manzan, S., 2007. Behavioral heterogeneity in stock prices. Journal of Economic Dynamics and Control 31, 1938–1970.

Boudt, K., Croux, C., Laurent, S., 2011. Robust estimation of intraweek periodicity in volatility and jump detection. Journal of Empirical Finance 18, 353–367.

Brock, W., Hommes, C.H., 1997. A rational route to randomness. Econometrica 69, 1059–1095.

Brock, W., Hommes, C.H., 1998. Heterogeneous beliefs and routes to chaos in a simple asset pricing model. Journal of Economic Dynamics and Control 22, 1235–1274.

Calvet, L.E., Fisher, A.J., 2007. Multifrequency news and stock returns. Journal of Financial Economics 86, 178–212.

Carr, P., Geman, H., Madan, D.B., Yor, M., 2002. The fine structure of asset returns: An empirical investigation. Journal of Business 75, 305–332.

Chauveau, T., Subbotin, A., 2013. Price dynamics in a market with heterogeneous investment horizons and boundedly rational traders. Journal of Economic Dynamics and Control 37, 1040 – 1065.

Cont, R., Tankov, P., 2004. Financial modelling with jump processes. Chapman & Hall/CRC Financial Mathematics Series, London.

Crouse, M.S., Nowak, R.D., Baraniuk, R.G., 1998. Wavelet-based statistical signal processing using hidden Markov models. IEEE Transactions on Signal Processing 46, 886–902.

De Grauwe, P., Kaltwasser, P.R., 2012. Animal spirits in the foreign exchange market. Journal of Economic Dynamics and Control , 11761192.

Dewachter, H., Erdemlioglu, D., Gnabo, J.Y., Lecourt, C., 2014. The intra-day impact of communication on euro-dollar volatility and jumps. Journal of International Money and Finance 43, 131–154.

Dieckmann, S., Gallmeyer, M., 2005. The equilibrium allocation of diffusive and jump risks with heterogeneous agents. Journal of Economic Dynamics and Control 29, 1547–1576.

Dominguez, K.M., 2006. When do central bank interventions influence intra-daily and longer-term exchange rate movements? Journal of International Money and Finance 25, 1051–1071.

Drechsler, I., Yaron, A., 2011. What's vol got to do with it? Review of Financial Studies 24, 1–45.

Duan, J.C., Yeh, C.Y., 2010. Jump and volatility risk premiums implied by VIX. Journal of Economic Dynamics and Control 34, 2232–2244.

Durand, J.B., Gonçalvès, P., 2001. Statistical inference for hidden Markov tree models and application to wavelet trees. Technical Report. Statistical Inference for Industry and Health, INRIA. Technical Report 4248.

Ederington, L.H., Lee, J.H., 1993. How markets process information: News releases and volatility. Journal of Finance 48, 1161–1191.

Ederington, L.H., Lee, J.H., 1995. The short-run dynamics of the price adjustment to new information. Journal of Financial and Quantitative Analysis 30, 117–134.

Fagan, S., Gençay, R., Xue, Y., 2013. Jump detection with wavelets for high-frequency financial time series. Quantitative Finance, forthcoming.

Fatum, R., Hutchison, M.M., 2003. Is sterilised foreign exchange intervention effective after all? An event study approach. Economic Journal 113, 390–411.

Fatum, R., Hutchison, M.M., 2006. Effectiveness of official daily foreign exchange market intervention operations in Japan. Journal of International Money and Finance 25, 199–219.

Gençay, R., Gradojevic, N., Selçuk, F., Whitcher, B., 2010. Asymmetry of information flow between volatilities across time scales. Quantitative Finance 10, 895–915.

Gençay, R., Selçuk, F., Whitcher, B., 2001. An introduction to wavelets and other filtering methods in finance and economics. Academic Press, San Diego.

Hommes, C.H., 2006. Heterogeneous agent models in economics and finance, in: Tesfatsion, L., Judd, K.L. (Eds.), Handbook of Computational Economics. Elsevier. volume 2 of *Handbook of Computational Economics*. chapter 23, pp. 1109–1186.

Hommes, C.H., 2011. The heterogeneous expectations hypothesis: some evidence from the lab. Journal of Economic Dynamics and Control 35, 1–24.

Hommes, C.H., Sonnemans, J., Tuinstra, J., van de Velden, H., 2005. Coordination of expectations in asset pricing experiments. Review of Financial Studies 18, 955–980.

Jacod, J., Todorov, V., 2008. Testing for common arrival of jumps in discretely-observed multidimensional processes. Annals of Statistics 37, 1792–1838.

Jong, d.E., Verschoor, W.F.C., Zwinkels, R.C.J., 2009. Behavioral heterogeneity and shift-contagion: Evidence from the asian crisis. Journal of Economic Dynamics and Control 33, 1929–1944.

Lahaye, J., Laurent, S., Neely, C.J., 2011. Jumps, cojumps and macro announcements. Journal of Applied Econometrics 26, 893–921.

Lee, S.S., Hannig, J., 2010. Detecting jumps from Lévy jump-diffusion processes. Journal of Financial Economics 96, 271–290.

Lee, S.S., Mykland, P.A., 2008. Jumps in financial markets: A new nonparametric test and jump dynamics. Review of Financial Studies 21, 2535–2563.

Lynch, P.E., Zumbach, G., 2003. Market heterogeneities and the causal structure of volatility. Quantitative Finance 3, 320–331.

Maheu, J.M., McCurdy, T.H., Zhao, X., 2013. Do jumps contribute to the dynamics of the equity premium. Journal of Financial Economics 110, 457–477.

Mandelbrot, B.B., 1974. Intermittent turbulence in self-similar cascades: divergence of high moments and dimension of the carrier. Journal of Fluid Mechanics 62, 331–358.

Neely, C.J., 1999. Target zones and conditional volatility: the role of realignments. Journal of Empirical Finance 6, 177–192.

Neely, C.J., 2011. A survey of announcement effects on foreign exchange volatility and jumps. Federal Reserve Bank of St. Louis Review 93, 361–385.

O'Hara, M., 2014. High-frequency trading and its impact on markets. Financial Analysts Journal 70, 18–27.

Percival, D.B., Walden, A.T., 2000. Wavelet methods for time series analysis. Cambridge Press, Cambridge.

Todorov, V., Tauchen, G., 2011. Volatility jumps. Journal of Business and Economic Statistics 29, 356–371.

Zhang, B.Y., Zhou, H., Zhu, H., 2009. Explaining credit default swap spreads with the equity volatility and jump risks of individual firms. Review of Financial Studies 22, 5099–5131.

Table 1: Descriptive statistics on the identified realized jumps

	EUR/USD	UST	EUB	DJI	SPI
Critical Level: $\alpha = 0.1$					
Panel A: Sample Description					
# of Total observations	572256	152178	219456	155532	155688
# of Dyadic observations	524288	131072	262144	131072	131072
# of Sample days	1987	1951	2032	1994	1996
# of Jumps	980	243	422	207	218
# of Jump-days	739	234	378	190	199
Panel B: Jump Counts					
# of (+) Jumps	500	111	178	108	107
# of (−) Jumps	480	132	244	99	111
% of (+) Jumps	51.02	45.68	42.18	52.17	49.08
% of (−) Jumps	48.98	54.32	57.82	47.83	50.92
Panel C: Probabilities					
P(Jump-days)(%)	37.19	11.99	18.60	9.53	9.97
P(Jumps)(%)	0.17	0.16	0.19	0.13	0.14
P((+)Jumps)(%)	0.09	0.07	0.08	0.07	0.07
P((−)Jumps)(%)	0.08	0.09	0.11	0.06	0.07
Panel D: Moment Ratios					
E(jumpsize|jumps)	0.23	0.40	0.18	0.38	0.36
E(jumpsize|jumps>0)	0.24	0.36	0.17	0.37	0.37
E(jumpsize|jumps<0)	-0.23	-0.44	-0.18	-0.40	-0.36
$\sigma(jumpsize \mid jumps)$	0.18	0.47	0.18	0.31	0.28
$\sigma(jumpsize \mid jumps > 0)$	0.20	0.39	0.16	0.28	0.26
$\sigma(jumpsize \mid jumps < 0)$	0.16	0.52	0.18	0.35	0.29

Notes: The table reports the summary statistics of the realized jumps detected by the rule given in Equation (4) in the main text. The sample covers the periods from January 1, 2002 to December 31, 2009. The significance level for the jump detections is $\alpha = 0.10$. EUR/USD: the EUR/USD exchange rate; UST: 30-year US Treasury bond future; EUR: 10-year Euro bond futures; DJI: Dow Jones index, SPI: S&P 500 index. In Panel A, the number of dyadic observations is equal to $N = 2^j$ and the length depends on the asset class ($j = 19$ for EUR/USD, $j = 18$ for EUB, $j = 17$ for DJI and UST).

Table 2: Translation of wavelet scales for financial assets

	Investment Time Horizons			
Scale	Minutes	Hours	Days	Years
1	10–20	.	.	.
2	20–40	.	.	.
3	40–80	0.7–1.3	.	.
4	.	1.3–2.7	.	.
5	.	2.7–5.3	.	.
6	.	5.3–10.7	.	.
7	.	10.7–21.3	.	.
8	.	21.3–42.7	0.9–1.8	.
9	.	.	1.8–3.6	.
10	.	.	3.6–7.1	.
11	.	.	7.1–14.2	.
12	.	.	14.2–28.4	.
13	.	.	28.4–56.8	.
14	.	.	56.8–113.7	.
15	.	.	113.7–227.5	.
16	.	.	227.5–455.1	0.62–1.25
17	.	.	.	1.25–2.49

Notes: The table presents the translation of wavelet scales into appropriate time horizons for the UST high-frequency jump series at 5-minutes sampling frequency. Each scale of the DWT corresponds to a frequency interval, or conversely an interval of periods, and thus each scale is associated with a range of time horizons.

Table 3: Estimated jump transition probabilities for the US Treasury bond futures

Scales	Low-to-Low	Low-to-High	High-to-High	High-to-Low
mean	0.916	0.085	0.545	0.454
p-value	(0.000)	-	(0.253)	-
median	0.948	0.051	0.502	0.497
p-value	(0.001)	-	(1.000)	-
std	0.028	0.094	0.125	0.125

Notes: The table reports the estimates of the jump risk transition probabilities. *mean* (*median*) denotes the mean (median) value for the conditional probabilities across various time scales, and *std* is the the standard deviation of the estimates across scales. Conditional probabilities $p_{0,j}$ and $p_{1,j}$ (at scale j given a jump state at scale $j+1$; $j = 7 \dots 17$) are from the scale-dependent transition matrices A_j in the wavelet hidden Markov tree (HMT) model for UST jump series. The p-values are given for the two-tailed t-tests for the equality of means (hypotheses H_0^A, H_0^B) and the two-tailed sign tests for the equality of medians (hypotheses H_0^C, H_0^D). The sample covers the periods from January 1, 2002 to December 31, 2009. Corresponding dyadic observations for the estimation of the model are given in Table 1.

Table 4: Estimated (positive and negative) jump transition probabilities for the US Treasury bond futures

Scales	Low-to-Low	Low-to-High	High-to-High	High-to-Low
		Positive (right-tail) jumps		
mean	0.929	0.070	0.500	0.499
p-value	(0.000)	-	(0.993)	-
median	0.981	0.018	0.523	0.476
p-value	(0.001)	-	(1.000)	-
std	0.112	0.112	0.234	0.234
		Negative (left-tail) jumps		
mean	0.935	0.064	0.548	0.451
p-value	(0.000)	-	(0.238)	-
median	0.966	0.034	0.512	0.487
p-value	(0.001)	-	(1.000)	-
std	0.104	0.104	0.126	0.126

Notes: The table reports the estimates of the positive and negative jump risk transition probabilities (upper panel and lower panel, respectively). *mean* (*median*) denotes the mean (median) value for the conditional probabilities across various time scales, and *std* is the the standard deviation of the estimates across scales. Conditional probabilities $p_{0,j}$ and $p_{1,j}$ (at scale j given a jump state at scale $j+1$; $j = 7 \dots 17$) are from the scale-dependent transition matrices A_j in the wavelet hidden Markov tree (HMT) model for UST jump series. The p-values are given for the two-tailed t-tests for the equality of means (hypotheses H_0^A, H_0^B) and the two-tailed sign tests for the equality of medians (hypotheses H_0^C, H_0^D). The sample covers the periods from January 1, 2002 to December 31, 2009. Corresponding dyadic observations for the estimation of the model are given in Table 1.

Table 5: Estimated jump transition probabilities for the Euro-bond futures

Scales	Low-to-Low	Low-to-High	High-to-High	High-to-Low
		All jumps		
mean	0.909	0.090	0.589	0.410
p-value	(0.000)	-	(0.084)	-
median	0.922	0.077	0.563	0.436
p-value	(0.001)	-	(0.065)	-
std	0.091	0.091	0.154	0.154
		Positive (right-tail) jumps		
mean	0.934	0.065	0.513	0.486
p-value	(0.000)	-	(0.647)	-
median	0.975	0.024	0.478	0.521
p-value	(0.001)	-	(0.548)	-
std	0.083	0.083	0.093	0.093
		Negative (left-tail) jumps		
mean	0.903	0.096	0.540	0.459
p-value	(0.000)	-	(0.104)	-
median	0.944	0.055	0.512	0.487
p-value	(0.001)	-	(0.065)	-
std	0.100	0.100	0.074	0.074

Notes: The table presents the estimates of jump risk transition probabilities across scales. Upper panel: all jumps, middle panel: positive jumps, lower panel: negative jumps. *mean* (*median*) denotes the mean (median) value for the conditional probabilities across various time scales, and *std* is the the standard deviation of the estimates across scales. Conditional probabilities $p_{0,j}$ and $p_{1,j}$ (at scale j given a jump state at scale $j+1$; $j = 7 \dots 17$) are from the scale-dependent transition matrices A_j in the wavelet hidden Markov tree (HMT) model for EUB jump series. The p-values are given for the two-tailed t-tests for the equality of means (hypotheses H_0^A, H_0^B) and the two-tailed sign tests for the equality of medians (hypotheses H_0^C, H_0^D). The sample covers the periods from January 1, 2002 to December 31, 2009. Corresponding dyadic observations for the estimation of the model are given in Table 1.

Table 6: Estimated jump transition probabilities for the Dow Jones index

Scales	Low-to-Low	Low-to-High	High-to-High	High-to-Low
		All jumps		
mean	0.871	0.128	0.474	0.525
p-value	(0.000)	-	(0.725)	-
median	0.967	0.032	0.495	0.504
p-value	(0.001)	-	(1.000)	-
std	0.165	0.165	0.229	0.229
		Positive (right-tail) jumps		
mean	0.902	0.098	0.520	0.479
p-value	(0.000)	-	(0.448)	-
median	0.979	0.020	0.514	0.485
p-value	(0.001)	-	(1.000)	-
std	0.151	0.151	0.086	0.086
		Negative (left-tail) jumps		
mean	0.926	0.073	0.464	0.535
p-value	(0.000)	-	(0.336)	-
median	0.991	0.008	0.493	0.507
p-value	(0.001)	-	(1.000)	-
std	0.121	0.121	0.115	0.115

Notes: The table presents the estimates of jump risk transition probabilities across scales. Upper panel: all jumps, middle panel: positive jumps, lower panel: negative jumps. *mean* (*median*) denotes the mean (median) value for the conditional probabilities across various time scales, and *std* is the the standard deviation of the estimates across scales. Conditional probabilities $p_{0,j}$ and $p_{1,j}$ (at scale j given a jump state at scale $j+1$; $j = 7 \dots 17$) are from the scale-dependent transition matrices A_j in the wavelet hidden Markov tree (HMT) model for DJI jump series. The p-values are given for the two-tailed t-tests for the equality of means (hypotheses H_0^A, H_0^B) and the two-tailed sign tests for the equality of medians (hypotheses H_0^C, H_0^D). The sample covers the periods from January 1, 2002 to December 31, 2009. Corresponding dyadic observations for the estimation of the model are given in Table 1.

Table 7: Estimated jump transition probabilities for the S&P 500 index

Scales	Low-to-Low	Low-to-High	High-to-High	High-to-Low
		All jumps		
mean	0.889	0.110	0.554	0.445
p-value	(0.000)	-	(0.229)	-
median	0.968	0.031	0.520	0.479
p-value	(0.001)	-	(0.065)	-
std	0.131	0 .131	0.141	0.141
		Positive (right-tail) jumps		
mean	0.902	0.097	0.513	0.486
p-value	(0.000)	-	(0.635)	-
median	0.985	0.014	0.521	0.478
p-value	(0.001)	-	(0.226)	-
std	0.170	0.170	0.094	0.094
		Negative (left-tail) jumps		
mean	0.933	0.067	0.493	0.506
p-value	(0.000)	-	(0.906)	-
median	0.985	0.014	0.507	0.492
p-value	(0.001)	-	(0.548)	-
std	0.116	0.116	0.183	0.183

Notes: The table presents the estimates of jump risk transition probabilities across scales. Upper panel: all jumps, middle panel: positive jumps, lower panel: negative jumps. *mean* (*median*) denotes the mean (median) value for the conditional probabilities across various time scales, and *std* is the the standard deviation of the estimates across scales. Conditional probabilities $p_{0,j}$ and $p_{1,j}$ (at scale j given a jump state at scale $j+1$; $j = 7 \ldots 17$) are from the scale-dependent transition matrices A_j in the wavelet hidden Markov tree (HMT) model for S&P 500 jump series. The p-values are given for the two-tailed t-tests for the equality of means (hypotheses H_0^A, H_0^B) and the two-tailed sign tests for the equality of medians (hypotheses H_0^C, H_0^D). The sample covers the periods from January 1, 2002 to December 31, 2009. Corresponding dyadic observations for the estimation of the model are given in Table 1.

Table 8: Estimated jump transition probabilities for the EUR/USD exchange rate

Scales	Low-to-Low	Low-to-High	High-to-High	High-to-Low
		All jumps		
mean	0.886	0.113	0.517	0.482
p-value	(0.000)	-	(0.528)	-
median	0.930	0.069	0.495	0.504
p-value	(0.001)	-	(1.000)	-
std	0.121	0.121	0.088	0.088
		Positive (right-tail) jumps		
mean	0.918	0.081	0.522	0.477
p-value	(0.000)	-	(0.365)	-
median	0.973	0.026	0.503	0.496
p-value	(0.001)	-	(0.548)	-
std	0.116	0.116	0.077	0.077
		Negative (left-tail) jumps		
mean	0.934	0.065	0.537	0.462
p-value	(0.000)	-	(0.241)	-
median	0.980	0.019	0.505	0.494
p-value	(0.001)	-	(0.065)	-
std	0.077	0.077	0.100	0.100

Notes: The table presents the estimates of jump risk transition probabilities across scales. Upper panel: all jumps, middle panel: positive jumps, lower panel: negative jumps. *mean* (*median*) denotes the mean (median) value for the conditional probabilities across various time scales, and *std* is the the standard deviation of the estimates across scales. Conditional probabilities $p_{0,j}$ and $p_{1,j}$ (at scale j given a jump state at scale $j+1$; $j = 7 \ldots 17$) are from the scale-dependent transition matrices A_j in the wavelet hidden Markov tree (HMT) model for the EUR/USD exchange rate jump series. The p-values are given for the two-tailed t-tests for the equality of means (hypotheses H_0^A, H_0^B) and the two-tailed sign tests for the equality of medians (hypotheses H_0^C, H_0^D). The sample covers the periods from January 1, 2002 to December 31, 2009. Corresponding dyadic observations for the estimation of the model are given in Table 1.

Table 9: Descriptive statistics on the jumps in the S&P 500 and VIX index

	SPI	VIX
Critical Level: $\alpha = 0.1$		
Panel A: Sample Description		
# of Total observations	126594	126516
# of Sample days	1623	1622
# of Jumps	203	694
# of Jump-days	183	526
Panel B: Jump Counts		
# of (+) Jumps	96	354
# of (−) Jumps	107	340
% of (+) Jumps	47.29	51.01
% of (−) Jumps	52.71	48.99
Panel C: Probabilities		
P(Jump-days)(%)	11.28	32.43
P(Jumps)(%)	0.16	0.55
P((+)Jumps)(%)	0.08	0.28
P((−)Jumps)(%)	0.08	0.27
Panel D: Moment Ratios		
E(jumpsize|jumps)	0.36	2.07
E(jumpsize|jumps>0)	0.37	2.13
E(jumpsize|jumps<0)	-0.35	-2.00
$\sigma(jumpsize \mid jumps)$	0.29	1.41
$\sigma(jumpsize \mid jumps > 0)$	0.30	1.55
$\sigma(jumpsize \mid jumps < 0)$	0.28	1.25

Notes: The table reports the summary statistics of the realized jumps detected by the rule given in Equation (4) in the main text. The sample covers the periods from July 1, 2003 to December 31, 2009. The significance level for the jump detections is $\alpha = 0.10$. SPI: S&P 500 index; VIX: CBOE volatility index.

Table 10: Estimated jump transition probabilities for the VIX index

Scales	Low-to-Low	Low-to-High	High-to-High	High-to-Low
		All jumps		
mean	0.767	0.232	0.573	0.426
p-value	(0.002)	-	(0.074)	-
median	0.722	0.277	0.528	0.471
p-value	(0.065)	-	(0.065)	-
std	0.215	0.215	0.123	0.123
		Positive (right-tail) jumps		
mean	0.824	0.175	0.591	0.408
p-value	(0.000)	-	(0.096)	-
median	0.970	0.029	0.578	0.421
p-value	(0.001)	-	(0.112)	-
std	0.197	0.197	0.200	0.200
		Negative (left-tail) jumps		
mean	0.808	0.191	0.533	0.466
p-value	(0.001)	-	(0.552)	-
median	0.945	0.054	0.556	0.443
p-value	(0.011)	-	(1.000)	-
std	0.222	0.222	0.182	0.182

Notes: The table presents the estimates of jump risk transition probabilities across scales. Upper panel: all jumps, middle panel: positive jumps, lower panel: negative jumps. *mean* (*median*) denotes the mean (median) value for the conditional probabilities across various time scales, and *std* is the the standard deviation of the estimates across scales. Conditional probabilities $p_{0,j}$ and $p_{1,j}$ (at scale j given a jump state at scale $j+1$; $j = 7 \dots 17$) are from the scale-dependent transition matrices A_j in the wavelet hidden Markov tree (HMT) model for VIX jump series. The p-values are given for the two-tailed t-tests for the equality of means (hypotheses H_0^A, H_0^B) and the two-tailed sign tests for the equality of medians (hypotheses H_0^C, H_0^D). The sample covers the periods from January 1, 2002 to December 31, 2009. Corresponding dyadic observations for the estimation of the model are given in Table 1.

Table 11: Model components and characteristics of realized jumps

Asset	Brownian	Jumps	Jump activity	Jump frequency	Jump variation
EUR/USD	(+)	(+)	finite	0.146 (0.771)	20.89%
UST	(+)	(+)	finite	0.034 (0.384)	29.05%
EUB	(+)	(+)	finite	0.080 (0.556)	30.68%
DJI	(+)	(+)	finite	0.021 (0.268)	21.86%
SPI	(+)	(+)	finite	0.024 (0.285)	28.20%
VIX	(+)	(+)	finite	0.091 (0.705)	41.91%

Notes: The table summarizes the results of the model selection tests. We follow Aït-Sahalia et al. (2012) to determine which components are present in the data. The sample covers the periods from January 1, 2002 to December 31, 2009. In the table, (+) indicates that the component is present, while the term *finite* (in the third column) refers to the jump activity. The fourth and last column present the estimated parameter values for the frequency of jump activity (standard errors in parenthesis), and the price variation due to jumps, respectively. Activity that occurs finitely often—such as Poisson jumps—has an activity level of 0. Activity that occurs infinitely has a positive parameter (except Gamma and variance-gamma (VG) processes). Cauchy and Normal Inverse Gaussian (NIG) jumps imply that the frequency parameter is 1; Brownian motion is extremely active with parameter 2. The online appendix presents the details of the testing procedures.

Table 12: Robustness of conditional probabilities for the S&P 500 Index (to jump methods)

Scales	Low-to-Low	Low-to-High	High-to-High	High-to-Low
		All jumps **(BTL)**		
mean	0.902	0.097	0.550	0.449
p-value	(0.000)	-	(0.260)	-
median	0.978	0.021	0.535	0.464
p-value	(0.001)	-	(0.226)	-
std	0.130	0.130	0.139	0.139
		Negative (left-tail) jumps **(BTL)**		
mean	0.935	0.064	0.482	0.517
p-value	(0.000)	-	(0.773)	-
median	0.990	0.009	0.507	0.492
p-value	(0.001)	-	(1.000)	-
std	0.102	0.102	0.200	0.200
		All jumps **(LH)**		
mean	0.910	0.089	0.522	0.477
p-value	(0.000)	-	(0.427)	-
median	0.981	0.018	0.507	0.492
p-value	(0.001)	-	(0.548)	-
std	0.126	0.126	0.088	0.088
		Negative (left-tail) jumps **(LH)**		
mean	0.949	0.050	0.468	0.531
p-value	(0.000)	-	(0.411)	-
median	0.992	0.007	0.493	0.506
p-value	(0.001)	-	(0.548)	-
std	0.091	0.091	0.122	0.122

Notes: The table presents the estimates of (S&P 500 index) jump risk transition probabilities. The abbreviation "**BTL**" denotes the Bollerslev et al. (2013) methodology, while the abbreviation "**LH**" denotes the Lee and Hannig (2010) method for jump detection. The label "All jumps" refers to both positive and negative jumps combined, and the label "Negative" concerns only negative jumps. The mean value for the conditional probabilities across various time scales is denoted by *mean*, the median value by *median* and the standard deviation by *std*. Conditional probabilities $p_{0,j}$ and $p_{1,j}$ (at scale j given a jump state at scale $j+1$; $j = 7 \dots 17$) that were used are from the scale-dependent transition matrices A_j in the wavelet hidden Markov tree (HMT) model for the S&P 500 Index jump series. The p-values are given for the two-tailed t-tests for the equality of means (hypotheses H_0^A, H_0^B) and the two-tailed sign tests for the equality of medians (hypotheses H_0^C, H_0^D). The sample covers the periods from January 1, 2002 to December 31, 2009. Corresponding dyadic observations for the estimation of the model are given in Table 1.

Table 13: Robustness of conditional probabilities for the S&P 500 Index (to sample)

Scales	Low-to-Low	Low-to-High	High-to-High	High-to-Low
		All jumps **(period: 2002−2013)**		
mean	0.885	0.114	0.501	0.498
p-value	(0.000)	-	(0.954)	-
std	0.178	0.178	0.098	0.098
		Negative (left-tail) jumps **(period: 2002−2013)**		
mean	0.927	0.072	0.550	0.449
p-value	(0.000)	-	(0.167)	-
std	0.093	0.093	0.113	0.113
		All jumps **(period: 2002−2006)**		
mean	0.874	0.125	0.558	0.441
p-value	(0.000)	-	(0.139)	-
std	0.172	0.172	0.114	0.114
		Negative (left-tail) jumps **(period: 2002−2006)**		
mean	0.920	0.079	0.535	0.464
p-value	(0.000)	-	(0.328)	-
std	0.128	0.128	0.109	0.109
		All jumps **(period: 2006−2009)**		
mean	0.929	0.070	0.555	0.444
p-value	(0.000)	-	(0.285)	-
std	0.095	0.095	0.153	0.153
		Negative (left-tail) jumps **(period: 2006−2009)**		
mean	0.919	0.080	0.461	0.538
p-value	(0.000)	-	(0.398)	-
std	0.153	0.153	0.138	0.138

Notes: The table presents the estimates of (S&P 500 index) jump risk transition probabilities for extended sample and sub-samples. The label "All jumps" refers to both positive and negative jumps combined and the label "Negative" concerns only negative jumps. The mean value for the conditional probabilities across various time scales is denoted by *mean* and the standard deviation by *std*. Conditional probabilities $p_{0,j}$ and $p_{1,j}$ (at scale j given a jump state at scale $j+1$; $j = 7 \dots 17$ for the extended sample, 2002−2013, and $j = 7 \dots 16$ for the sub-samples: 2002−2006 and 2006−2009) that were used are from the scale-dependent transition matrices A_j in the wavelet hidden Markov tree (HMT) model for the S&P 500 Index jump series. The p-values are given for the two-tailed t-tests for the equality of means (hypotheses H_0^A, H_0^B). Corresponding dyadic observations for the estimation of the model are given in Table 1.

Table 14: Reversed conditional probabilities for the S&P 500 Index

Scales	Low-to-Low	Low-to-High	High-to-High	High-to-Low
		All jumps		
mean	0.939	0.060	0.072	0.927
p-value	(0.000)	-	(0.000)	-
median	0.991	0.008	0.007	0.992
p-value	(0.002)	-	(0.002)	-
std	0.154	0.154	0.158	0.158
		Negative (left-tail) jumps		
mean	0.943	0.056	0.053	0.946
p-value	(0.000)	-	(0.000)	-
median	0.994	0.005	0.000	1.000
p-value	(0.002)	-	(0.002)	-
std	0.155	0.155	0.157	0.157

Notes: The table presents the estimates of (S&P 500 index) jump risk transition probabilities for the reversed direction of jump risk, i.e., from high- to low-frequencies. The label "All jumps" refers to both positive and negative jumps combined and the label "Negative" concerns only negative jumps. The mean value for the conditional probabilities across various time scales is denoted by *mean* and the standard deviation by *std*. Conditional probabilities $p_{0,j}$ and $p_{1,j}$ (at scale $j+1$ given a jump state at scale j; $j = 7 \ldots 17$) that were used are from the scale-dependent transition matrices A_j in the wavelet hidden Markov tree (HMT) model for the S&P 500 Index jump series. The p-values are given for the two-tailed t-tests for the equality of means (hypotheses H_0^A, H_0^B). Corresponding dyadic observations for the estimation of the model are given in Table 1.

Figure 1: Realized jumps over time at pre-determined time scale

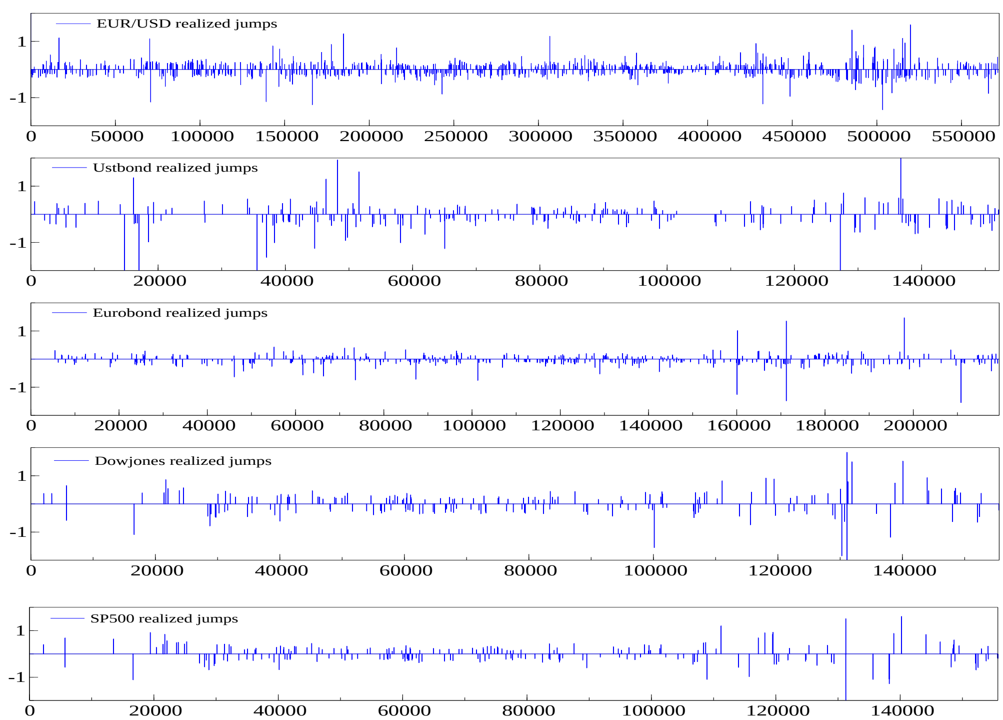

Notes: The figures plot the arrival times and sizes of realized jumps based on the rule given in Equation (4). The sample covers the periods from January 1, 2002 to December 31, 2009. The significance level for the jump detection is $\alpha = 0.10$.

Figure 2: Sequence of jump states from the fitted wavelet-HMT model for all realized jumps of UST

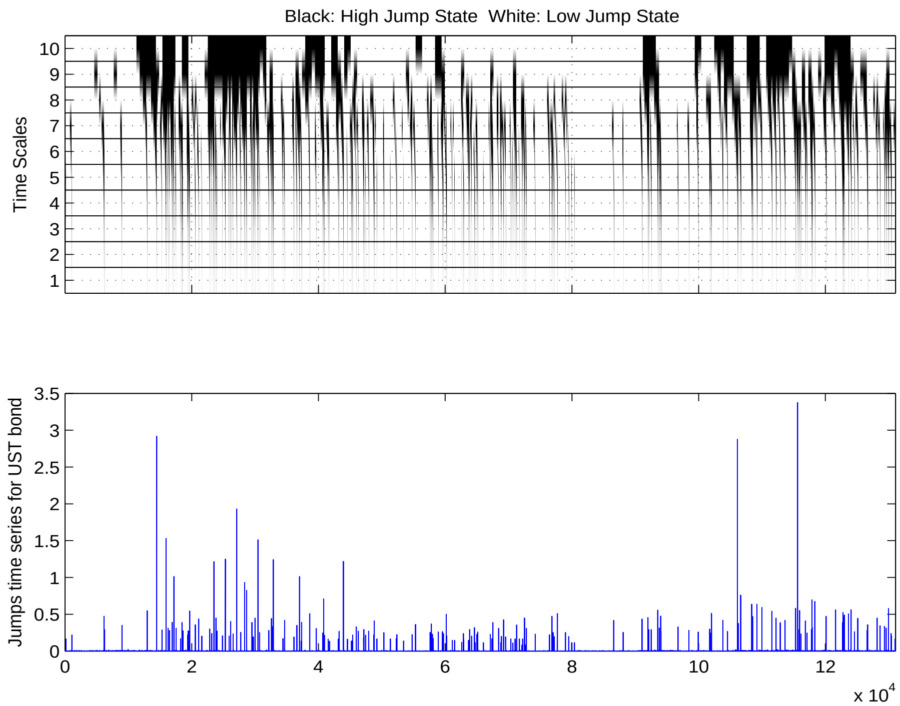

Notes: The first state $S = 0$ (light rectangles) indicates a low jump risk (state) regime and the second state $S = 1$ (dark rectangles) indicates a high jump risk regime. The figure demonstrates the sequence of states for all jumps (i.e., positive + negative) in absolute values. X-axis denotes time and the sample covers the periods from January 1, 2002 to December 31, 2009.

Figure 3: Sequence of jump states from the fitted wavelet-HMT model for positive and negative realized jumps of UST

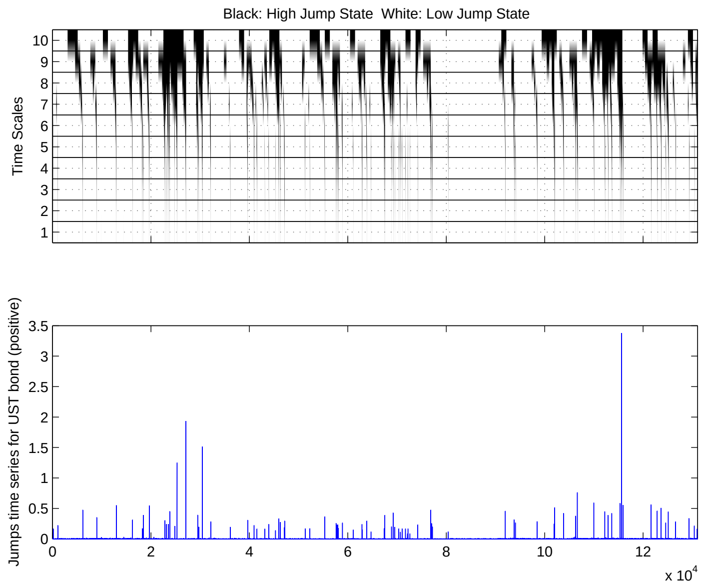

Panel A

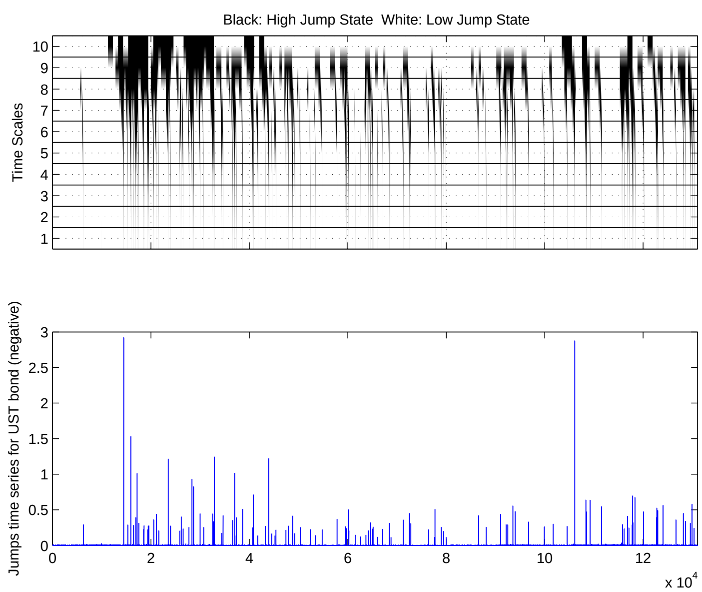

Panel B

Notes: The first state $S = 0$ (light rectangles) indicates a low jump risk (state) regime while the second state $S = 1$ (dark rectangles) indicates a high jump risk regime. Panel A: Only positive jumps; Panel B: only negative jumps (in absolute values). X-axis denotes time and the sample covers the periods from January 1, 2002 to December 31, 2009.

Figure 4: S&P 500 and VIX on September 29, 2008

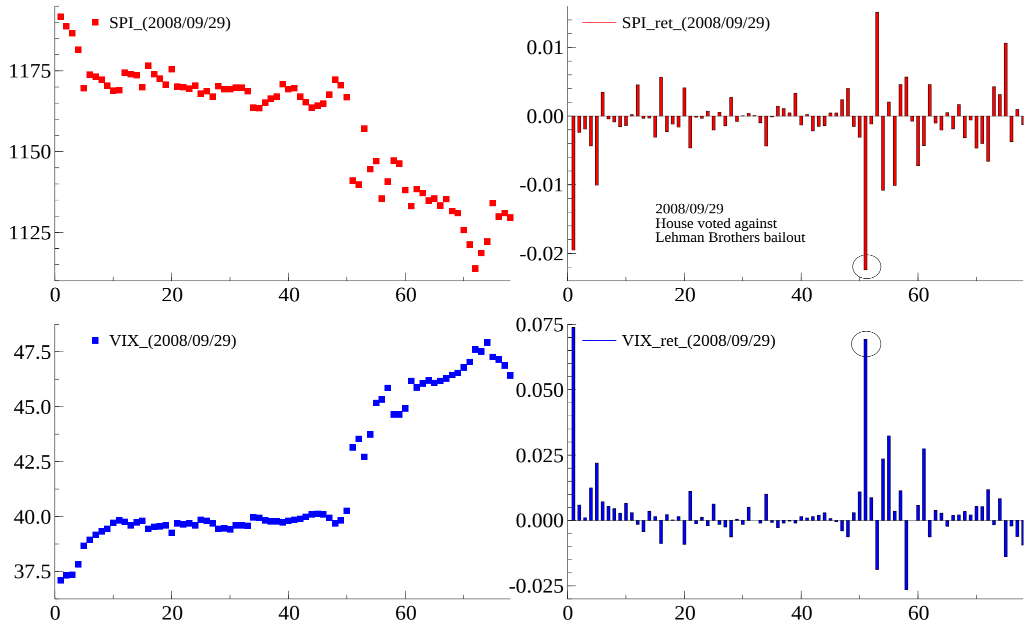

Notes: Illustration of a jump in the VIX index when House voted against the bailout of Lehman Brothers on September 29, 2008: 5-minute intra-day prices (left panels) and log-returns (right panels). The circles on the right panels indicate a detected jump occurring simultaneously around 17:40 GMT.

Figure 5: Flash crash: S&P 500 and VIX on May 6, 2010

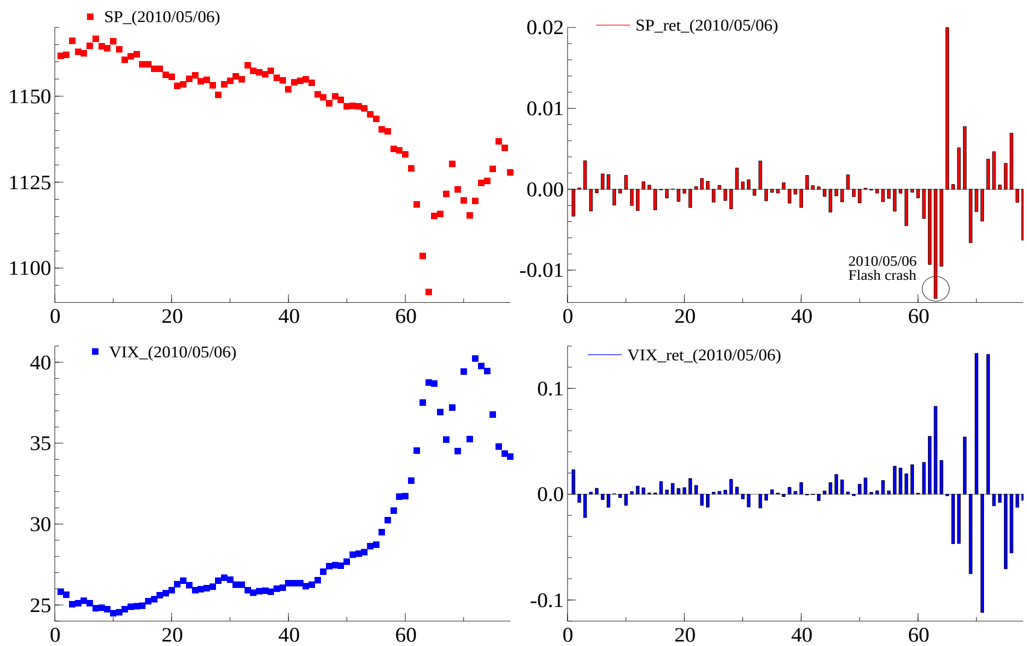

Notes: Illustration of a sequence of jumps in the VIX index and S&P 500 on May 6, 2010 when Flash crash occurred at 19:45 GMT: 5-minute intra-day prices (left panels) and log-returns (right panels). The circle on the upper right panel indicates a detected jump occurring in the S&P 500 index around 19:45 GMT.

Figure 6: Sequence of jump states from the fitted wavelet-HMT model for all realized jumps of VIX

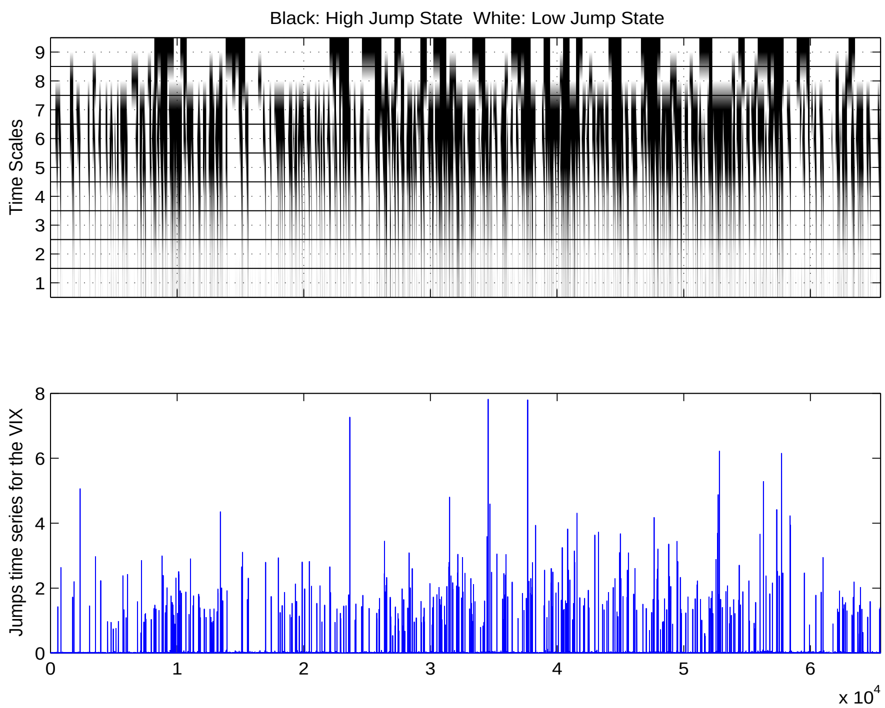

Notes: The first state $S = 0$ (light rectangles) indicates a low jump risk (state) regime while the second state $S = 1$ (dark rectangles) indicates a high jump risk regime. The figure demonstrates the sequence of states for all jumps (i.e., positive + negative) in absolute values. X-axis denotes time and the sample covers the periods from January 1, 2002 to December 31, 2009.